

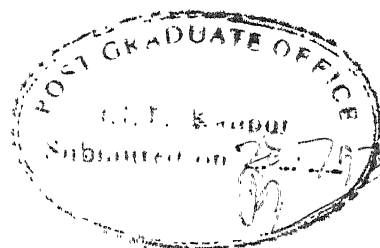
SYNTHESIS AND CHARACTERIZATION OF
Na-A ZEOLITE USING DIATOMACEOUS CLAY

A Thesis Submitted
In Partial Fulfilment of the Requirements
for the Degree of
MASTER OF TECHNOLOGY

by
BISWAJIT GHOSH

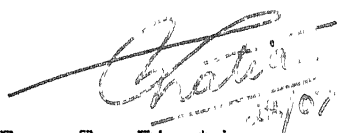
to the
Materials Science Programme
INDIAN INSTITUTE OF TECHNOLOGY KANPUR
JULY, 1992

Dedicated
to
My Parents

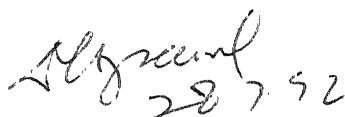


CERTIFICATE

This is to certify that the present work entitled "SYNTHESIS AND CHARACTERIZATION OF Na-A ZEOLITE USING DIATOMACEOUS CLAY" has been carried out by Biswajit Ghosh under our supervision and that this work has not been submitted elsewhere for a degree.

A handwritten signature in cursive script, appearing to read "S. Bhatia", with the date "28/7/92" written below it.

Dr. S. Bhatia
Professor
Department of Chemical Engg.
Indian Institute of Technology
Kanpur - 208 016

A handwritten signature in cursive script, appearing to read "D.C. Agrawal", with the date "28/7/92" written below it.

Dr. D.C. Agrawal
Professor
Materials Science Programme
Indian Institute of Technology
Kanpur - 208 016

1 - OCT 1932

114318

MSP-1992-M-BIS-SYN

ACKNOWLEDGEMENTS

I express my deep sense of gratitude to my thesis supervisors, Dr.D.C. Agrawal and Dr.S. Bhatia for providing timely guidance, valuable advice and constructive criticism at each stage of this investigation. Their keen interest and constant encouragement have enabled me to accomplish this work satisfactorily in the stipulated period.

Help recieved from Mr. J.S. Virdi, Mr.R. Khanna, Mr.A.K. Ganguly, Mr. P.K.Pal, Mr. Umashankar and Mr. Ahmed at various stages of work is appreciated.

The help rendered by Prasanta, Atanu, Sonu, Santanu, Ajju, Mogambo, Bhandarkar, Rama Rao, Tommy will be remembered for ever.

Special thanks are also due to all staff of MSP and ACMS for their help and coperation.

BISWAJIT

CONTENTS

	PAGE
Subject	
List of Tables	(iv)
List of Figures	(vi)
Abstract	
1. INTRODUCTION	1
2. STATEMENT OF THE PROBLEM	26
3. EXPERIMENTAL PROCEDURES	29
4. RESULTS AND DISCUSSIONS	38
5. CONCLUSIONS AND RECOMMENDATIONS	82
6. REFERENCES	87
7. APPENDIX	90

LIST OF TABLES

TABLE		PAGE
1.1	Some important patents on the synthesis of Zeolite A	13
1.2	Some typical chemical compositions of several brands of diatomite (32)	17
1.3	Zeolite IR Assignments, Cm^{-1} [9]	21
1.4	Comparative study of zeolite A with other builder material [5]	25
3.1	Chemical composition of supplied diatomaceous clay	30
3.2	Experimental parameters used in particle size analysis	35
4.1	First order response surface strategy (First Move)	44
4.2	The 2^{6-2} First order (First Move) Design Matrix and Values of the Responses	47
4.3	First order Response Surface Strategy (First Move) Test for the Adequacy of the Model for % crystallinity	50

4.4	First order Response Surface Strategy (First Move) : Test for the Adequacy of the Model for % Yield	51
4.5	First order Response Surface Strategy (Second Move) : Test for the adequacy of the Model for % yield	53
4.6	First order Response Surface Strategy (First Move) : Calculaiton of Path of Steepest Ascent	57
4.7	First order Response Surface Strategy (First Move) : Result of Experiments along the path of Steepest Scent	58
4.8	X-ray Powder data for Na-A-Zeolite	69
4.9	X-ray data for Zeolite P _c .	70
4.10	X-ray Powder data for zeolite HS	71
4.11	Particle Size Analysis ;by Coulter- Counter Method	75
4.12	Surface Areas of Synthesized Zeolite A	78

LIST OF FIGURES

FIGURE		PAGE
1.1	Primary building blocks of Zeolites	4
1.2	SBU of Zeolites	4
1.3	Truncated Octahedra	7
1.4	The framework of Sodalite	7
1.5	Schematic representation of aluminosilicate gel crystallization	11
3.1	Line diagram of the autoclave assembly	31
4.1	Effect of Silica, Alumina ratio on Zeolite A Crystallization and Yield at 95°C for 30 hours $\left(\frac{H_2O}{Al_2O_3} = 210\right)$	60
4.2	Effect of Reaction temperature on Zeolite A Crystallization and Yield at SiO_2/Al_2O_3 (Molar) ratio 1.25 for 30 hours $\left(\frac{H_2O}{Al_2O_3} = 210\right)$	61
4.3	Effect of Reaction time on Zeolite A Crystallization and Yield at 95°C at SiO_2/Al_2O_3 (Molar) ratio	62

1.25 and 30 hours $\left(\frac{\text{H}_2\text{O}}{\text{Al}_2\text{O}_3} = 2:10\right)$

4.4	X-ray Pattern of Diatomaceous clay	65
4.5	X-ray Pattern of Standard Zeolite 4A	66
4.6	X-ray Patterns of Synthesized Zeolite A	67
4.7	X-ray Patterns ;of Synthesized Zeolite A	68
4.8	Infra-red Spectra of Synthesized Zeolites	73
4.9	Infra-red Spectra of Standard (4A) Zeolite	74
4.10	Particle Size Analysis of Synthesized Zeolite	76
4.11	Calcium break through Curve from Zeolite A	80
4.12	Calcium and Magnesium breakthrough Curves from zeolite A	81
4.13	SEM Photographs of Synthesized Zeolite sample	85
4.14	High magnification SEM of synthesized Zeolite sample	86

ABSTRACT

Na-A Zeolite was prepared by hydrothermal syntehsis using diatomaceous clay. The composition and process variables e.g. reaction temperature, reaction time, pH and

molar ratios of reactants $\left(\frac{\text{SiO}_2}{\text{Al}_2\text{O}_3}, \frac{\text{Na}_2\text{O}}{\text{SiO}_2} \text{ and } \frac{\text{H}_2\text{O}}{\text{Al}_2\text{O}_3} \right)$ were

optimized using Fractional Factorial Designs. Percentage crystallinity as optimized by Surface Methodology Technique was found to be 92%.

The Synthesized Zeolites were characterized using X-ray diffraction, Infra-red Spectroscopy, and Scanning Electron Microscopy. The average particle size and surface area were measured by Coulter Counter and BET Surface Technique respectively. Microstructure reveals different morphologies for Na-A Zeolite and Zeolite HS. While Na-A Zeolite exhibited spheroidal particles, Zeolite HS were of equidimensional polyhedral crystal of cubic symmetry.

Ion exchange properties were studied for the zeolite samples. The calcium exchange capacity of zeolite sample in hard water was found as 5.4 meq Ca^{+2}/gm of zeolite. The

result indicates that this zeolite can be used as a ;building agent in the detergent formulation.

INTRODUCTION

The properties and uses of zeolites are being explored in many scientific disciplines such as inorganic and organic chemistry, physical chemistry, colloid chemistry, bio-chemistry and in all types of chemical engineering process technology. Zeolites are used commercially in various applications such as hydrogen drying, hydrocarbon sweetening, ethylene purification, in soap detergent and cosmetic industry and many other fields. Due to their large industrial applications synthesis of zeolite is important. Zeolites are known as molecular sieves because of their selective adsorption behaviour. The dehydrated zeolite crystals act as sieves by the selective adsorption or the rejection of gas/liquid molecules due to the difference in the sizes and structural characteristics of such materials. The internal pore space available in zeolite are governed by the individual zeolite structure.

As early as in 1756, Cronsted, a Swedish mineralogist observed that the mineral stilbite gave off steam when heated. This result led him to coin the term 'Zeolite' which is derived from the two Greek words 'Zeo' (to boil) and Lithos

(stone). Today it is known that zeolites are hydrated crystalline tectosilicates [1].

McBain [24] first defined porous solid materials which exhibit the sieving properties on the molecular scales. Zeolite molecular sieves have uniform pore size, uniquely determined by the lattice structure of the crystal. The pores completely exclude molecules, which are larger than their diameter. Zeolites have high internal surface area available for adsorption due to channels or pores which uniformly penetrate the entire volume of the solid. The external surface of the adsorbent particles contributes only a small amount of the total available surface area. The availability of wide range of particle sizes, porosities and ion exchange properties of zeolites is beneficial for using them as detergent builder.

1.1 STRUCTURE OF ZEOLITES

Crystalline Zeolite molecular sieves are chemically and structurally complex materials comprising silicates on major group (2). The fundamental building block of all zeolites is a tetrahedron of four oxygen anions surrounding an interstitial silicon or aluminium ion. These tetrahedra are

arranged in such a way that each of the four oxygen anions is shared, in turn, with another silica or alumina tetrahedron. The crystal lattice extends in three dimensions. Each silicon ion has its +4 charge balanced by the four tetrahedral oxygens, and the silica tetrahedra are therefore electrically neutral. Each alumina tetrahedra has a residual charge of -1 since the trivalent aluminium ion is bonded to four oxygen anions. Thus each alumina tetrahedron requires a +1 charge from a cation in the structure to maintain electrical neutrality. The primary building blocks of zeolite are indicated in Fig. 1.1. These metal cations which neutralize the excess anionic charge on the aluminosilicate framework are usually alkali metal and alkaline earth metal cations and at least some of them must be able to undergo reversible ion-exchange if the material is to be classified as a zeolite.

The silica and alumina tetrahedra are combined into more complicated secondary units, which form the secondary building blocks of the zeolite framework crystal structure (Fig. 1.2). Tectosilicates do have in general $\frac{\text{Si}}{\text{Al}}$ ratio < 1 . This implies that an aluminium atom can not have another aluminium atom in its second co-ordination. Loewenstein (1954) was the first to rationalize this ratio in terms of the Al-O-Al avoidance rule [3]. The silica and alumina tetrahedra are geometrically

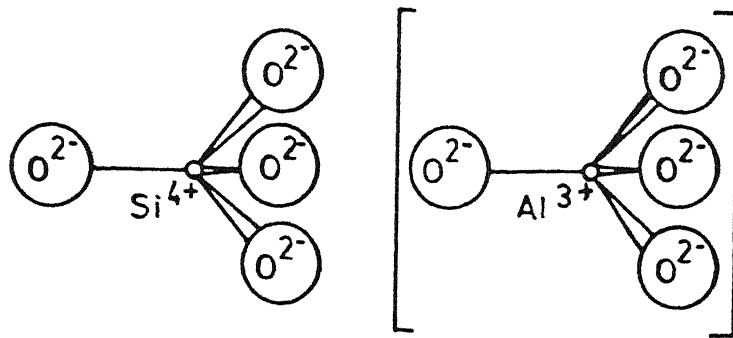
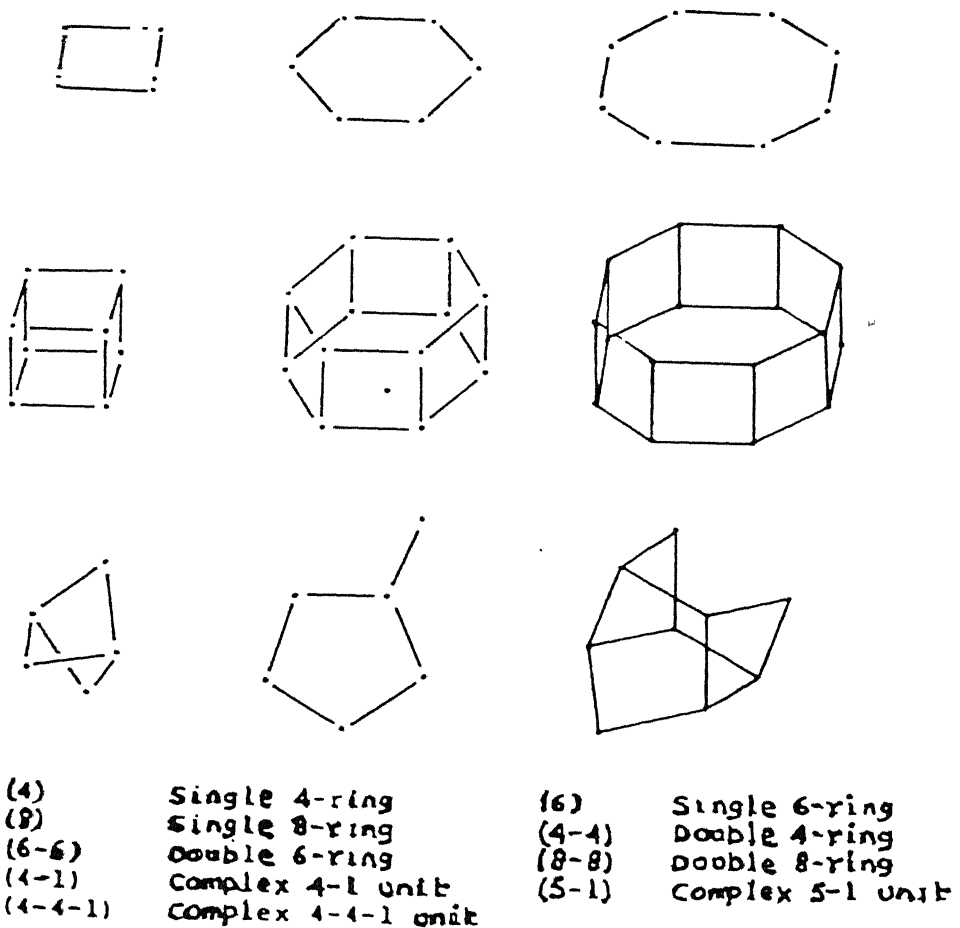
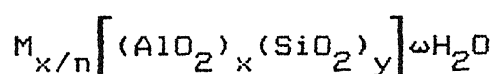


Fig. 1.1 : Primary building blocks of zeolite

Group	Secondary Building Unit (SBU)
1	Single 4-ring, S4R
2	Single 6-ring, S6R
3	Double 4-ring, D4R
4	Double 6-ring, D6R
5	Complex 4-1, T_5O_{10} unit
6	Complex 5-1, T_8O_{16} unit
7	Complex 4-4-1, $T_{10}O_{20}$ unit



arranged. Since the aluminosilicate frame work is hydrophilic, it absorbs moisture from ambient air into its voids. The formula for the unit cell is written as,



where M is the cation with valency n, balancing the negative charge with the framework aluminium ions. The metal cations, which neutralize the excess anionic charge on the aluminosilicate framework are usually alkali metal and alkaline earth metal cations. W is the number of water molecules which fill the remaining volume in the interstices of tetrahedra per unit cell. The ratio y/x ranges from 1 to 10 for natural and synthetic zeolites. The three dimensional framework of zeolite consists of channels and inter connected voids or cages. The void spaces are occupied by cations and water molecules. The intracrystalline zeolite water can be removed commonly by thermal treatment reversibly without affecting the structure and channels and voids become vacant except for the remaining cations. The pore structure varies greatly from one zeolite to another. In all zeolites, pore diameters are determined by the free aperture resulting from 4,6,8,10 or 12 member rings of oxygen atoms, and these have

maximum values calculated to be 2.6, 3.4, 4.2, 6.3, and 7.4 Å, respectively. Because of puckering of apertures, the effective free aperture of the pore structure may some what be reduced and the aperture may be elliptical [4].

1.2 STRUCTURE OF ZEOLITE A

The primary building block of all the zeolites are same, formed by alumina and silica tetrahedra. Secondary building block and their connection is different, in different type of zeolites.

In zeolite-A, the silica and alumina tetrahedra are joined together to form a cuboctahedron as show in Fig. (1.3). This unit, referred to as a sodalite unit or truncated octahedron, contains 24 silica and alumina tetrahedra and is secondarybuilding block for zeolite A. When truncated octahedra are connected by bridge oxygen atoms between the four-membered rings, zeolite A is formed as shown in figure (1.4).

The free pore aperture of zeolite A is determined by an eight membered oxygen ring and therefore has a free-pore diameter of 4.2 Å. The resultant cavity enclosed by the eight sodalite units has a free dimension large enough to inscribe

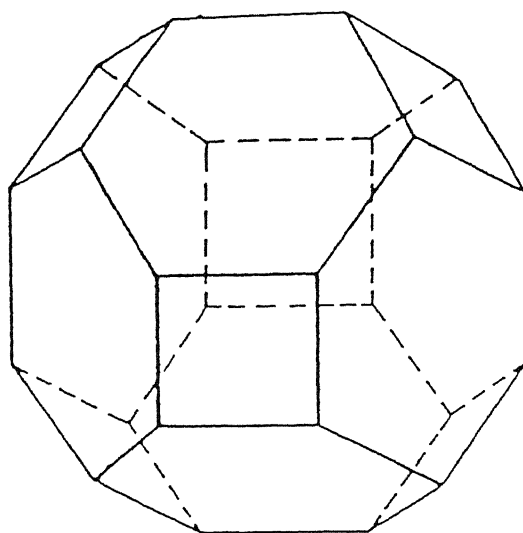


Fig. 1.3 : Truncated octahedra

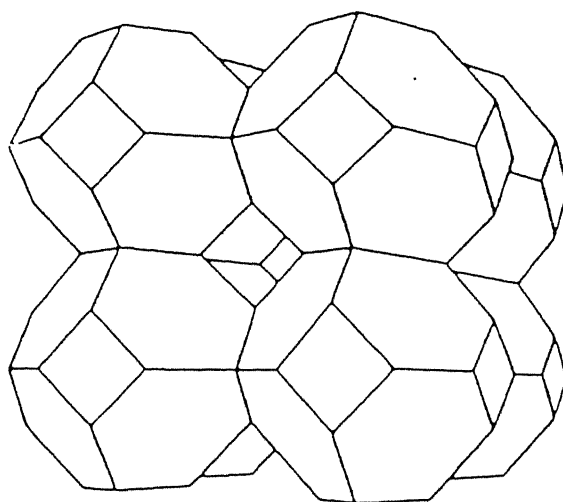


Fig. 1.4 : The framework of sodalite

on 11.4 Å sphere. There are two three-dimensional pore structures, one involving the interconnected supercages separated by 4.2 Å minimum pore apertures and the other consisting of the sodalite units alternating with supercages and having 2.6 Å free pore aperture.

1.3 SYNTHESIS OF ZEOLITES

Methods of synthesis and various aspects of the synthesis and crystallization of zeolite A are reviewed in the following paragraphs.

1.3.1 Principle of Synthesis

The crystallization of zeolite is consistent with the simplicity principle proposed by Goldsmith [6] which relates the ease of crystallization to structural simplicity. Goldsmith defines high 'Simplicity' as being synonymous with disorder structural simplicity or high entropy".

The growth of crystalline aluminosilicate such as zeolite first requires the formation of a nucleus. In a system of high disorder the principle favours the formation and development of the nucleus with highest simplicity, which may be the nucleus of a crystal of metastable phase (7).

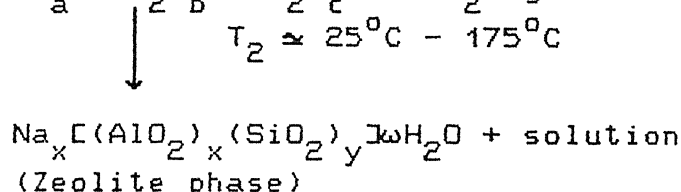
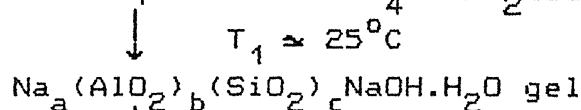
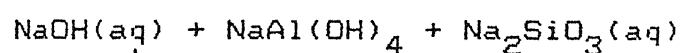
General Conditions for synthesis of zeolites

Figure 1.5 shows a general scheme for the synthesis of zeolite starting from clay material. The general conditions for the synthesis of zeolites are as follows :

- (1) Reactive starting material such as freshly co-precipitated or amorphous solid.
- (2) Relatively high pH introduced in the form of an alkali metal hydroxide or other strong base.
- (3) Low temperature hydrothermal condition with concurrent low autogeneous pressure at saturated water vapour pressure.
- (4) A high degree of supersaturation of the components of the gel leading to nucleation of a large number of crystals.

The gels are crystallized in a closed hydrothermal system at temperature varying generally from room temperature to about 175°C. In some cases high temperatures (upto 300°C) are used. The pressure is generally the autogeneous pressure approximately equivalent to the saturated vapour pressure (SVP) of water. The time required for crystallization varies from few hours to several days. For the $\text{Na}_2\text{O}-\text{Al}_2\text{O}_3-\text{SiO}_2-\text{H}_2\text{O}$

system, the gel preparation and crystallization are represented schematically as follows :



1.3.2 SYNTHESIS OF ZEOLITE A

As pointed out earlier, hydrothermal process of synthesis of zeolite is most widely accepted one. Most synthetic zeolites including zeolite A are produced under non-stable conditions and must be considered as a metastable phase in thermodynamic sense. Zeolite A is usually synthesized from different Clay materials such as Kaolinite, Halloysite, Montmorillonite etc. Zeolite A can be prepared from Korean Feldspar, meta kaolin and even from slag of furnaces melting aluminium. In Japan, zeolite A has been synthesized from local clays by companies like Nippon Chem Co. & Toyo Soda manufacturing company Ltd. for use as detergent builder. Marinox & company workers have chalked out procedures for producing low iron content zeolite A, which is extremely suitable for detergent builder.

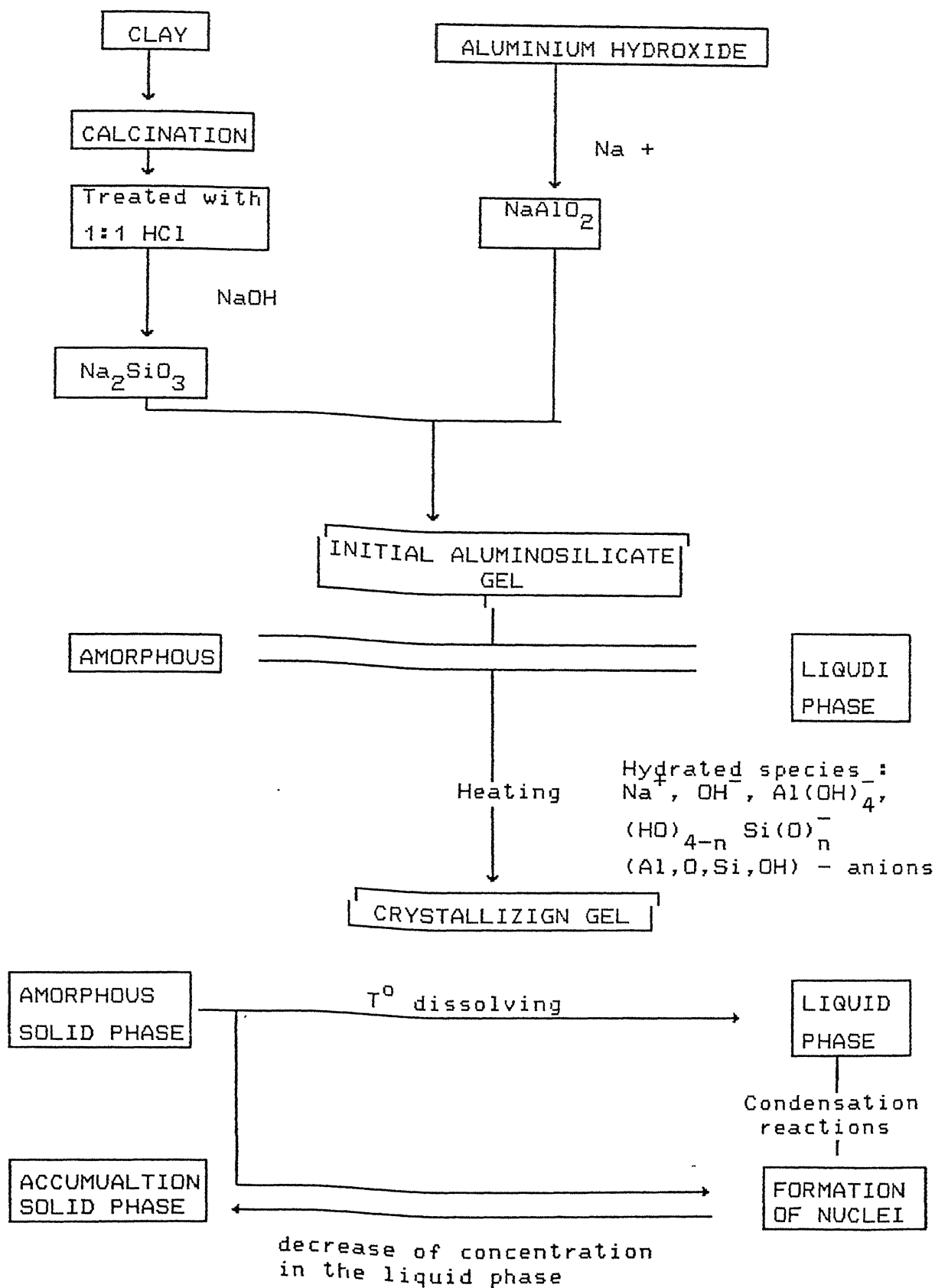


Fig. 1.5 Schematic representation of aluminosilicate gel crystallization

The hydrothermal synthesis of zeolite results in a large number of framework structures (25). Synthesis of zeolites has been reported using Non aqueous solvents such as hexanol, glycol, sulfolane [26,27].

The solvent and inorganic cation have an important structure-directing effect in this systems, yet organic cations did not seem to influence the zeolite growth process (26,27). It has been proposed that the cation-water complex as well as the structure of water plays an important role in zeolite nucleation (28,29). Addition of solvents to an aqueous system can perturb these structure and, therefore, provides a method to evaluate their role in zeolite synthesis.

Bowers and Dutta (30) reported the synthesis of zeolite A and X using solvents such as HMPA and DMSO with a typical composition of $8.6 \text{ Na}_2\text{O} \cdot 1.5 \text{ SiO}_2 \cdot 0.75 \text{ Al}_2\text{O}_3 \cdot x \text{ solvent} \cdot y \text{ H}_2\text{O}$.

Table 1.1 presents important patents for the synthesis of zeolite A starting from different materials.

Table 1.1 Some important patents on the synthesis of zeolite A

<u>Reactants and their Composition</u>	<u>Temp.</u>	<u>Time</u>	<u>Remarks</u>
1. Sodium aluminate solution containing 20.5 Al_2O_3 & 20.1 wt% Na_2O contacted with Sodium Silicate solution having 28.9% SiO_2 [Chemical Abstract Vol. 110, p 1956 & 7, Year 1989]	95°C	30min	Avg. particle dia $5.5\mu\text{m}$ & 83% crystalline.
2. Raw Source was waterglass obtained from volcanic glass. 215 gm pulverized volcanic glass, 197 ml 48% NaOH & 503 ml H_2O heated at 100°C for 4 hrs to prepare (I), 600 ml 48% NaOH & 77.3 gm 95% solid NaOH & 604.8 gm Industrial $\text{Al}(\text{OH})_3$ were heated at 100°C for 1 hrs to make (II) Solution, mixing of 350 ml (I) & 78.8 ml (II) Solution [Chemical Abstract, Vol. 104, p 151796, Year 1986]	-		Zeolite A crystallization 80%; suitable for detergent builder.

3. A Sod. aluminate solution - - Product has prepared from mixing 138 gm 85% crystallinity ; zeolite A content was 100% ; so very suitable for detergent.
- 92% $\text{Al}(\text{OH})_3$ to 670 ml water containing 360 gm NaOH at 80°C was treated at 35°C with 332 gm Na-Silicate (SiO_2 28% , Na_2O 10%, H_2O 62%) stirred at 70% achieved. Filtered Cake containing 40% solids treated with 50 gm 6% NaOH & dried at 150°C
- [Chemical Abstract, Vol. 101, p. 221217, Year 1984]
4. Very fine commercial clay 180°C 5hrs dia 3.1 μm with iron content (Fe_2O_3) 0.33% at 800°C Calcination temp, Kaolin was reacted with Cl_2 gas. Chlorinated calcination reduced Fe_2O_3 0.05%, Calcination period 8 hrs. There after clay added

with 10% NaOH solution.

Molar ratio were 1.25

$\text{Na}_2\text{O}:1.0 \text{ Al}_2\text{O}_3:2\text{SiO}_2:40\text{H}_2\text{O}$

[Chemical Abstract, Vol.

105, p.193379, Yr. 1986)

5. 0.1 mol sodium metasilicate 95°C 25 hrs Zeolite A with
($\text{Na}_2\text{SiO}_3 \cdot 9\text{H}_2\text{O}$) dissolved in trace of zeol-
100 gm H_2O . 40gm (0.1 mol) ite P_c .

aluminium hydroxide was
added to it.

[Chemical Abstract, Vol. 96,

p 219645, p 220053, Year

1982)

6. Mix of Burnt Kaolin 10.0, - 48 hrs Zeolite A
NaOH 9.1, & H_2O 75.6 gm was obtained.
heated to 50°C

[Chemical Abstract, Vol. 97,

p. 200-281, Yr. 1982)

1.3.3 Zeolite can be synthesized using different clay source. One of the source could be Diatomaceous clay :

Diatomaceous earth which is known under numerous designation such as diatomite, Kieselguhr, tripolite, fossil flour etc. It consists of siliceous remains of microscopic aquatic organism known as diatoms. Individual diatoms may vary in length from 0.005 to 0.4 mm.

The world's largest and purest deposits of diatomite are probably those occurring in the United States in the Lompoc area, 50 miles north-west Santa Barbara, California operated by the Great Lakes Carbon Corporation and Johnson Manville Company.

The purest form of diatomaceous earth is composed chiefly of opaline silica, but in most commercial deposits the material contains impurities such as quartz, sand, clay, iron oxide, carbonates of lime and magnesia, organic or carbonaceous material, so that content of diatomaceous silica rarely exceeds 85 percent.

Diatomite is marketed in three general forms i.e natural, calcined and flux calcined. The natural product has been dried, ground and if necessary air classified.

Table 1.2 Some typical chemical composition of several brands of diatomite [32]

	I	II	III	IV
SiO_2	89.6	88.9	71.	95.48
Al_2O_3	4.0	3.12	16.0	1.15
Fe_2O_3	1.5	1.61	1.0	1.45
TiO_2	0.2	0.16	-	0.14
CaO	0.5	0.4		0.14
MgO	0.6	0.78	9.0	Trace
Na_2O	3.3	4.91		0.49
K_2O				0.38
Water				
Soluble material	0.15	-	-	-
Moisture	0.1	-	2.0	0.21

1.4 CHARACTERIZATION OF ZEOLITE A

A complete characterization of a zeolite involves the work on the framework structure, cation content, chemical composition and various structure-related properties like the ion-exchange behaviour and the physical adsorption characteristics. Thus to characterize a zeolite, several tools of analysis have to be used. These include the X-ray diffraction analysis, infrared absorption spectroscopy, scanning electron microscopy and particle size analysis in addition to many other conventional chemical techniques.

X-ray analysis has been used to determine the framework structure of zeolites, the crystallinity of zeolites, distribution of the cation sites and the structural change caused during ion-exchange, calcination etc.

The crystal framework is of cubic symmetry with a unit cell parameter of the synthesized material of 8.87 \AA . Jarman [8] reported a method for determining the silicon-aluminium ratio (Si/Al) from powder X-ray diffraction data for A-type of zeolite and it is to be expected that the X-ray diffraction patterns of other structure types will show a similar compositional dependence. Therefore, it is possible to apply

powder X-ray intensity ratios more generally to the analysis of framework composition of zeolite materials.

Zeolite structures can be classified according to the common elements of framework topology and the secondary zeolite structures are found in the secondary zeolite unit. By an extension of the infrared studies, it may be possible to deduce structural information on a new zeolite for which X-ray structural analysis is not complete. The non availability of large single crystals of synthetic zeolites limits the structural investigations using X-ray diffraction technique. The polyhedral building units present in the zeolite framework can be best understood with infrared (IR) spectroscopy. The mid infrared region ($1300-200\text{ cm}^{-1}$) of the spectrum is used since it contains the fundamental vibration of the framework $(\text{Si,Al})\text{O}_4$ tetrahedra. Infrared data for this region on synthetic zeolites (including A type zeolite) are available in the Literature [9,10]. The IR spectra of zeolites indicate peaks that can be assigned to (i) internal vibrations of the TO_4 tetrahedra, not sensitive to structural vibrations and (ii) vibration related to the linkages between the tetrahedra which are sensitive to overall structure [11]. These are presented in table 1.3. The number of Al atoms in the framework structure influence the variation of frequency in

both the assymmetric stretching in the region $970-1020\text{ cm}^{-1}$ as also the symmetric stretching in the region $670-720\text{ cm}^{-1}$ [9].

Removal of the zeolite water does not modify the IR spectra within the mid-infrared region of several synthetic zeolites containing alkali, metal ions [1,2,9]. The association of water molecules with the cation and/or the framework oxygen ions of a zeolite is dependent upon the openness of the structure. The three typical bond characteristics of hydrogen-bonded OH around 3400 cm^{-1} , the sharp bond typical of isolated OH at 3700 cm^{-1} and the usual bonding vibration of the water at 1645 cm^{-1} . The isolated OH stretching is attributed to the interaction of the water hydroxyl with the cation. The other bonds are assigned to the hydrogen bonding of water molecules to a surface oxygen and to the bonding made of water [12].

Table 1.3 Zeolite IR Assignments, cm^{-1} [9]

1.	Internal tetrahedra	Assymmetric stretch	1250-950
		Symmetric stretch	720-650
		T-O Bond	500-420
2.	External Linkages	Double rings	650-500
		Pore openings	420-300
		Symmetric stretch	820-750
		Asymmetric stretch	1150-1050

Synthetic zeolites that are crystallized from typical aqueous hydrogels are produced as crystalline powders with a typical particle size of a few microns under the electron microscope, these crystals may show well developed faces or may appear as irregular, highly twinned aggregates. In order to establish the shape & size of various synthesized zeolite scanning electron microscopy is necessary. As a supporting evidence for inferences drawn from X-ray diffraction patterns of various zeolite electron diffraction data of species and micrographs are essential.

1.4.1 APPLICATIONS

Although zeolites were discovered in 1756 their large scale commercial application did not begin until the 1950's. In 1959, Milton was the first to initiate large scale use of synthetic zeolite-A as adsorbents and catalysts. The zeolite 4A type is the most suitable in various zeolites because of its largest ion-exchange capacity. Zeolite with a smaller particle size is most suited because high ion-exchange rates are achieved at even lower temperature. Zeolite A has been used in the formulation of detergents [Ref. 5]. A particle size of $1\text{ }\mu\text{m}$ is very common. In heavy duty powder detergents commonly used for laundry washing, many ingredients are formulated together with the anionic surfactants consisting of main components. In such a complex system, in which zeolite is formulated as a builder, calcium ion exchange will occur through some routes in the water softening processes. As a solid-state zeolite softens water only by a heterogeneous cation exchange process, at the initial stage a part of calcium will react with carriers and anionic surfactants dissolved in the system to form their calcium-salts. Sodium salts will be released by ion exchange of calcium salts with the zeolite (5). In this process, one of the key points to get

good detergency depends on how soon anionic surfactants are reproduced into original sodium salts. Therefore, it is important to have obtaining a smaller zeolite particles in detergent formulation. It was also found that in washing performance tests, undesirable deposition of zeolite particles on washed fabrics were seen as white visible residues, especially on dark colored clothes. But it was found that this was caused by the deposition of large agglomerated particles of zeolite having diameters of above 10 μm . This problem can be solved by using strict control of the amounts of large size agglomerated particles. This will again favour the smaller particle size.

Zeolite A as detergent builder

Polycondensed phosphates, represented by sodium tripolyphosphate (STPP) were the most commonly used builders and they constituted the main ingredients together with surfactant materials in synthetic powder detergents for heavy duty laundry. The phosphates have important properties to improve cleaning efficiency by the effect of water softening through sequestration of calcium and magnesium ions and that of preventing soil redeposition. In addition to these important builder properties, STPP has also excellent effects

to improve physical properties of powder detergents, especially free-flowing property and strength of the particles. Therefore, if phosphate contents is simply reduced or eliminated, the powder detergent will suffer significant damages in their performance properties as well as cost. For phosphates, many materials have been studying including citrates, polyacrylates, maleic acid derivatives, nitrotriacetate (NTA), etc. As shown in the following tabel most of the selected products have some disadvantages. The keen interest was finally focussed on zeolite A (5).

Table 1.4 Comparative Study of Zeolite A with other builder material [Ref. 5]

Material	Calcium Ion Binding Amount	Cost position	Safety/Ecology
Sodium Citrate	Poor	Weak	Increased load on oxygen required for degradation
Sodium Phospho-acrylate	Excellent	Weak	Poor Biodegradability
Sodium polymaleate	Equivalent	Weak	Poor Biodegradability
Sodium nitrotri acetat	Excellent	Weak	Not yet cleared on safety
Zeolite A	Equivalent	Competitive/Strong	Harmless

CHAPTER-2

STATEMENT OF THE PROBLEM

Zeolite A finds extensive industrial application due to its small pore size, good ion exchange property, high thermal stability and unique channel structure.

In the earlier work on the synthesis of zeolite A, the starting materials for silica and alumina have been from pure chemical sources. Efforts have also been made by some workers to use clay minerals like kaolinite as a source of alumina and silica in the synthesis of synthetic zeolites. Efforts have not been made by any workers to synthesize zeolite A using diatomaceous clay as a source of silica and alumina.

Diatomaceous earth which is known under numerous designation such as diatomite, kieselguhr, tripolite, fossil-flour etc. is also sold under various trade name. It consists of siliceous remains of microscopic aquatic organism known as diatomite. Diatomite, as experiences in India reveal, is easily available in large quantities at an extremely low cost. This diatomite on complete calcination yields porous, cellular and high-grey coloured which on

analysis has been found to contain amorphous silica upto around 89% by weight of the clay. This clay can be pretreated with 1:1 HCl for complete removal of iron present in it. Being cellular this silica is in a highly reactive state.

As such diatomaceous clay is an important source of silica, which on leaching with an alkali, sodium-hydroxide offers great potentialities for its use in the synthesis of zeolite catalysts. In developing countries like India, the possibility of using this diatomite in the synthesis of zeolite offer a great potentiality.

All these considerations generate thoughts on the following lines :

- (1) Can synthesis of A-type zeolite be attempted using diatomaceous clay as a primary source of silica.
- (2) What are the optimum value of different parameters like $\frac{\text{SiO}_2}{\text{Al}_2\text{O}_3}$ (molar) ratio of the starting mixture, $\frac{\text{Na}_2\text{O}}{\text{SiO}_2}$ (mole) ratio of the starting mixture, temperature and time of the formation of zeolite and their role.
- (3) What are the different bonds present in the synthesized zeolite, Do they match with standard zeolite?

- (4) What are the phases present in synthesized zeolite and impurities.
- (5) What are the particle sizes of synthesized zeolite?
- (6) Is it possible to use these synthesized zeolite A as a detergent builder?

Using design of experiments methodology an attempt has been made in present work to find out the optimum values of the different parameters needed for the synthesis of zeolite A. Various characterization techniques such as X-ray diffraction, Infrared spectroscopy, SEM, particle size measurement are used.

Ion exchange properties useful in the detergent formulation of the synthesized zeolite are also determined. The information generated in the present study will be useful for the synthesis of zeolite material as detergent builder from cheap sources of silica.

CHAPTER-3

EXPERIMENTALPROCEDURES

3.1 MATERIALS

In the present investigation diatomite, sodium hydroxide and aluminium hydroxide gel were used as the starting materials in the mixture for the synthesis of zeolite A.

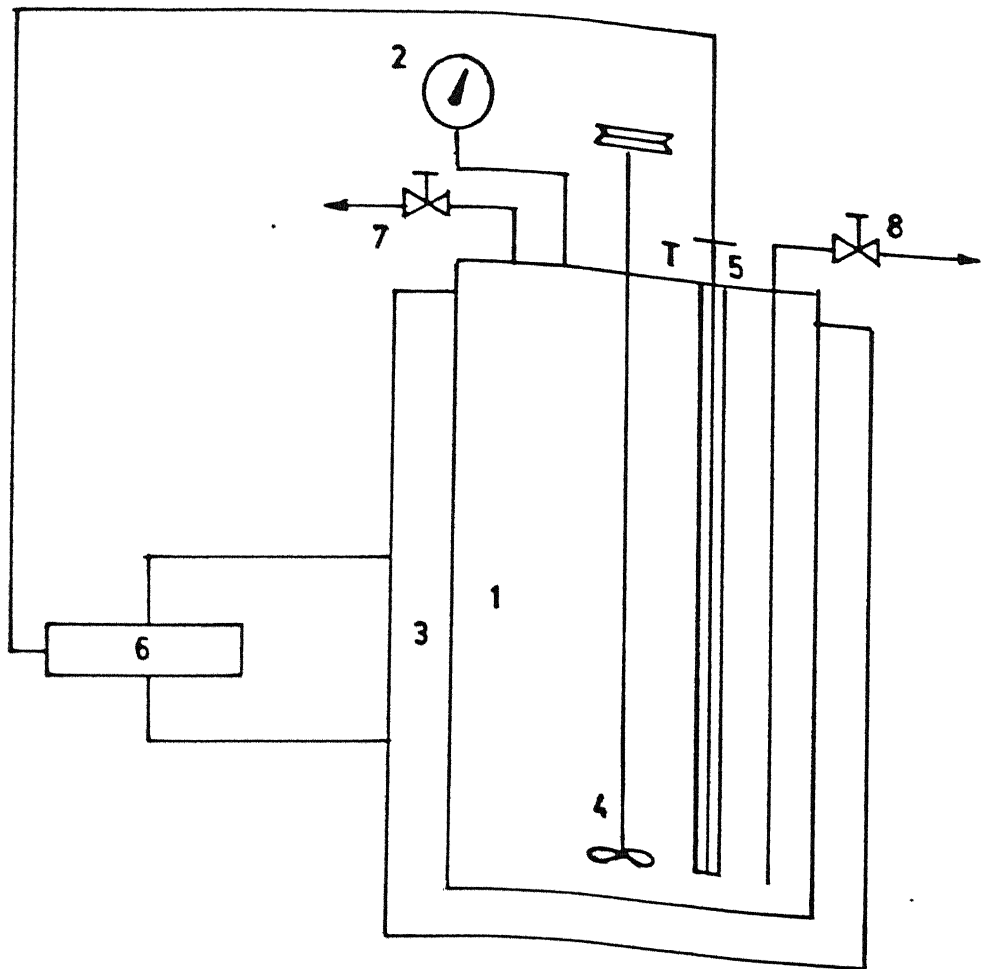
The sodium hydroxide was in the form of pellets (supplied by M/s Ranbaxy Laboratories, New Delhi) of 96.0 percent purity Aluminium hydroxide was supplied by M/s. Robert Johnson, Bombay. The diatomaceous clay was obtained from M/s Clays & Refractories, Jodhpur, Rajasthan. It was in the processed form and of 98% purity. Its chemical composition is show in Table 3.1. The method of analysis is described in Appendix.

Table 3.1 Chemical Composition of Supplied Diatomaceous Clay

Components	% by weight
Silica	82.5
Alumina	5.9
Water	10.4
Iron (as Fe ⁺³)	1.2
Calcium (as Ca ⁺²)	negligible
Magnesium (as Mg ⁺²)	negligible

3.2 EQUIPMENT

The reaction and crystallization was conducted in a high pressure Parr Reactor. This unit consists of a stainless steel vessel B of 1000 ml capacity, designed to withstand a pressure 2000 p.s.i. and a temperature of 350⁰C (Fig. 3.1). A motor driven stirrer S is provided. A gas release valve V₁ is provided to release the pressure in the reactor at the end of the run. The autoclave has temperature-indicator controller (Indotherm) together with an electrical heater assembly. This



- 1. Stainless steel vessel ; 2. Pressure gauge ;
- 3. Heating assy. ; 4. Stirrer ; 5. Thermocouple ;
- 6. Temp. controller ; 7. Gas release valve ;
- 8. Sampling valve.

FIG.3.1 LINE DIAGRAM OF THE AUTOCLAVE ASSY.

facility enables the control of the temperature of reaction mixture to an accuracy of $\pm 1^{\circ}\text{C}$.

3.3 DETAILS OF SYNTHESIS

Diatomite was first calcined to 900°C for 4 hrs, which is beyond the dehydroxylation range. Diatomite during this process loses the hydroxyl ions from its structure and the amorphous product formed. After calcination diatomite is treated with 1:1 HCl to remove iron. The requirement of silica was all met from diatomite itself and no other source was used for the same. Hence silica/alumina ratio during the reaction was maintained by adding additional alumina in the form of aluminium hydroxide to the reaction mixture of aluminosilicate gel.

The aluminosilicate was prepared by treating diatomite, aluminium hydroxide gel with aqueous NaOH solution and with continuous stirring by a magnetic stirrer for 8-10 hours at temperature ranging between $25-30^{\circ}\text{C}$. This reaction mixture was charged into the autoclave for hydrothermal reaction after adding required amount of water and raising the temperature to the requisite extent. At the end of each run conducted for a specific period of reaction, the product was centrifuged and washed thoroughly with distilled water so that there is no

sodium aluminate trapped in the pore of synthesized zeolite which is then oven-driven at 120°C for 7-8 hours.

In the synthesis, the temperature of reaction was varied from 90°C to 100°C. Products were obtained at different times ranging from 24 hours to 36 hours of reaction time. The $\frac{\text{SiO}_2}{\text{Al}_2\text{O}_3}$ (molar), ratio varied from 1 to 1.5. The $\frac{\text{H}_2\text{O}}{\text{Al}_2\text{O}_3}$ molar ratio was kept constant 210.

3.4 METHODS OF CHARACTERIZATION

The synthesized zeolites are characterized by different techniques like X-ray diffraction, IR spectroscopy, scanning electron microscopy etc. Surface area and particle size are measured by BET surface area measurement technique and Coulter-Counter technique respectively.

3.4.1 X-RAY DIFFRACTION

X-ray diffractograms were obtained with a diffractometer (Riech Seifert model) using Ni-filtered Cu-K α radiation. Scanning was done from 6° to 50° (2 θ) with a scanning speed 3°/min. The time constant and counts per second were maintained at 10 sec. and 10K (sometimes 5K also used) respectively. The exact peak positions were checked by

obtaining the counts from point to point within the peak range. The interplanar spacing (d) values were estimated from the peak (2θ) values for all synthesized samples and were compared with standard zeolite A. X-ray data for a standard zeolite A sample (4A molecular sieve type zeolite) was also recorded.

3.4.2 INFRARED SPECTROSCOPY

The infrared pattern for samples were recorded using a Perkin-Elmer 521 IR spectrometer using KBr-Pellet technique. The spectra was obtained in the range $4000-600\text{ cm}^{-1}$ which covers the frequency range for the framework structure and also for the associated water.

3.4.3 PARTICLE SIZE ANALYSIS

Particle size analysis of the synthesized zeolite powder was carried out using Coulter-Counter model Z_B and B (Coulter Electronics Ltd., England). A dual threshold method was used with the following experimental parameters.

Table 3.2 Experimental Parameters used in Particle Size Analysis

Electrolyte	:	NaCl
Aperture diameter	:	50 μm
Manometer volume	:	0.5 μL
Calibration factor	:	3.18
Dispersant	:	Coulter
Grain Control	:	5
Matching Switch	:	10

3.4.4 SCANNING ELECTRON MICROSCOPY

Morphology of the samples prepared in the present study was observed under JEOL JSM840 SC Scanning Electron Microscope (SEM) using an operating voltage of 25KV in the secondary electron mode at magnifications upto 2×10^4 . Specimens were coated with silver under a vacuum of 0.1 torr before they were scanned in the microscope. The silver coating ensures electrical conductivity across the areas of the specimen surface and prevents charge build up.

3.4.5 SURFACE AREA MEASUREMENT (BET SURFACE AREA)

The surface areas of the synthesized zeolites were measured with a QUANTASORB SORPTION APPARATUS, (MODEL NO. 08-7), using a single point method. Single point measurements were accomplished using only one composition of N_2 and He (30% N_2 and 70% He). Liquid Nitrogen was the cryogenic liquid. Only nitrogen gas was physically adsorbed at the liquid nitrogen temperature, the helium serving as an inert carrier.

The surface area and specific surface area were calculated using the following relations :

Surface Area

$$S_t = \left[1 - \frac{P}{P_0} \right] \times \frac{A}{A_c} \times V_c \times 4.03 \text{ m}^2$$

Specific Surface Area

$$S = \frac{S_t}{W} \text{ m}^2/\text{gm}$$

where, V_c = Cell volume, P & P_0 are Partial pressure of air and oxygen,

A = adsorbate volume, & A_c desorbed volume, m^3

W = weight of the sample, gm

3.5 ION EXCHANGE TEST

The calcium and magnesium exchange capacity was determined by contacting zeolite Na-A samples (synthesized) at 60°C with hard water solution, renewed five times over a two-week period. Analysis of calcium and magnesium ions present in the hard-water was performed using EDTA titration.

In dynamic exchange tests, glass columns (1.5 cm diameter) were loaded with 10 gm of zeolite powder (particle size 3.5 μm). The columns were operated down flow feeding at 5 to 10 cc/min of the solution. Cation concentration $\text{Ca}^{+2}/\text{Mg}^{+2}$ at the column outlet was determined by EDTA titration method.

The above test was conducted to determine the ion exchange properties of synthesized zeolite A which is to be used as detergent builder.

CHAPTER-4

RESULTS AND DISCUSSION

In the present study, synthesis of zeolite A and its characterization have been carried out, the results of which are presented in this chapter together with relevant discussion.

The present study can be categorized into three parts. In the first one, optimization studies of different variables like temperature, reaction time and the initial composition of the mixture are covered. The second part comprises of the characterization studies on the synthesized zeolite using X-ray diffraction, infrared spectroscopy, scanning electron microscopy and particle size analysis. In the third and final part ion exchange properties of the synthesized zeolite were tested as its possible application in the detergent formulation.

4.1 OPTIMIZATION STUDIES

In the present investigation, the optimum values of different variables were obtained in order to get maximum

crystallinity of zeolite sample. Effect of different variables like $\frac{\text{SiO}_2}{\text{Al}_2\text{O}_3}$ (mole) ratio, reaction temperature and time of reaction on % crystallinity and % yield of zeolite A were studied. % crystallinity and % yield are defined by

$$\% \text{ crystallinity} = \frac{\text{Area of the XRD peak of the product}}{\text{Area of the XRD peak of standard sample}} \times 100$$

$$\% \text{ yield} = \frac{\text{Molar weight of zeolite A formed}}{\text{Molar weight of aluminosilicate}} \times 100$$

Zeolite 4A is taken as standard for % crystallinity calculation

4.1.1 RESPONSE SURFACE METHODOLOGY

Response Surface Methodology (RSM) was used for this optimization study. This technique has been discussed elaborately by Kittrell and Erjavec (14), Box et al. (15), Davies (16), Khuri and Cornell (17).

Let Y be the response of a chemical process dependent on the levels of K factors X_1, X_2, \dots, X_k which can be precisely measured and controlled. The model for the u^{th} combination of factor levels is given by,

$$Y_u = \phi (X_{1u}, X_{2u}, \dots, X_{ku}) + \xi_u, \quad u = 1, 2, \dots, N \quad (4.1.1)$$

where, N is the number of experiments.

ϕ is the functional relationship,

and ξ is the error involved.

A geometrical portrait of the response function in the factor space is called a response surface. The experimental region R , is a bounded subspace of the whole factor space. The experimental region is bounded because of the practical limitations. The response surface methodology locates a point $(X_1^0, X_2^0, \dots, X_k^0)$ within the experimental region R , at which Y is an extremum (18,19,20). The traditional one factor-at a time method, where the experiments are conducted holding all the other factors constant often fails to locate the true optimum.

The response surface methodology cuts down the experimental effort by making use of experimental designs which permit the experimenter to assess the strength of the interactions between the factors while varying them simultaneously (19).

RSM consists of several steps

1. The first step is to design a set of experiments and conduct them to get reliable estimates of the parameters.

When the number of factors is small, factorial design can be used. On the other hand, fractional factorial designs are used when the number of factors are large. The details of factorial and fractional factorial designs are discussed by Box et al. (15) and Rao and Iyengar (21).

2. A suitable mathematical model is proposed to fit for the experimental data and then test for model adequacy through lack-of-fit F-tests (22).
3. To find out the optimum conditions of the independent variables which will produce the maximum (or minimum) value of the response. At a point which is remote from the optimum, there is a little curvature in the true response surface and first order models will be satisfactory to describe the response surface. In the vicinity of the optimum, however, higher order models will be required due to the presence of curvature in the response surface.

RSM is sequential in nature. Some experiments are carried out, valuable information is gathered and the next stage is designed for getting better values of the response. Generally the method of steepest ascent (or descent) is

applied for moving sequentially along the direction of maximum (or minimum) increase (or decrease) in response.

4.1.2.1 VARIABLES IDENTIFICATION AND THEIR LEVELS

Important variables which influence the percent crystallinity and yield of zeolite A are $\frac{\text{SiO}_2}{\text{Al}_2\text{O}_3}$ (molar) ratio, $\frac{\text{Na}_2\text{O}}{\text{SiO}_2}$ ratio, pH of the mixture, gel formation temperature, crystallization temperature & crystallization time. After knowing the important variables influencing the process, a base level had to be chosen within the experimental region. The base levels of the factors were chosen on the basis of an a-priori knowledge. Further the variation interval for each factor had to be chosen. The variation interval of a factor when added or subtracted from the base level gives the upper or the lower level of the factor respectively.

To simplify the recording of the conditions of an experiment, and the processing of the experimental data the values of the factors were coded as follows :

$$X_i = \frac{\bar{X}_i - \bar{X}_{10}}{V_i} \quad i = 1, 2, \dots, k, \quad (4.1.2)$$

where, X_i is the coded value of the i-th factor,
 \bar{X}_i is the natural value of the i-th factor,

\bar{X}_{i0} is the natural value of the base level of the i -th factor,

and V_i is the variation interval of the i -th factor.

Conventionally, the coded value of upper level corresponds to +1, the lower level to -1 and the base level to 0. The upper, lower and base levels of the variables in this first stage of design are given in Tabel 4.1.

The following dependent variables (responses) were considered to be important

- a. % crystallinity of zeolite A
- b. % yield of zeolite A.

of the above responses, % crystallinity of zeolite A was selected as the response to be optimized with respect to the independent variables. Though % yield of zeolite A was not optimized, data for this response was also processed and fitted to models to have information on the effect of different variables on % yield.

Table 4.1 First Order Response Surface Strategy (First Move)

LEVELS OF FACTORS

Factor	Code	Base level (-)	Lower level (-)	Higher level (-)
$\frac{\text{SiO}_2}{\text{Al}_2\text{O}_3}$ (mole) ratio in starting mix	X_1	1.25	1	1.5
$\frac{\text{Na}_2\text{O}}{\text{SiO}_2}$ (mole) ratio in starting mix	X_2	3.45	2.5	4.4
pH of reaction mixture	X_3	13.5	13	14
Temperature of hydrogel formation (°C)	X_4	37.5	25	50
Temperature of Crystallization (°C)	X_5	95	90	100
Reaction time (hours)	X_6	30	24	36

4.1.1.2.2 SELECTION OF EXPERIMENTAL DESIGN

Since there are six variables, a 2^{6-2} fractional factorial design around the base levels was employed. The design matrix is shown in Table 4.2. The basis for choosing $x_5 = x_1x_3$ and $x_6 = x_1x_4$ as these combinations are expected to have minimum interactions. Experiments were carried out in a randomized sequence to avoid bias, on the part of experimenter. The values of all the responses (% crystallinity, % yield) for the first move of experiments runs numbered 1 to 16) as planned in the design matrix are given in Table 4.2. Experiment No. 10 was repeated four times so as to obtain an estimate of the error.

4.1.1.2.3 MODEL FITTING

The following first order model has been fitted to the experimental data.

$$\hat{Y} = \hat{b}_0 + \hat{b}_1x_1 + \hat{b}_2x_2 + \hat{b}_3x_3 + \hat{b}_4x_4 + \hat{b}_5x_5 + \hat{b}_6x_6 \quad (4.1.3)$$

where $\hat{b}_0, \dots, \hat{b}_6$ are the best fitted values of coefficients, x_i is the i -th variable in its coded form and \hat{Y} is the predicted

value of the response. The coefficients can be estimated by the least squares technique as

$$\hat{\underline{b}} = (\underline{X}^T \underline{X})^{-1} \underline{X}^T \underline{Y} \quad (4.1.4)$$

Table 4.2 The 2^{6-2} First Order (First Move) Design Matrix and values of the Responses

Run No.	Factors in coded form						Values of responses	
	X_1	X_2	X_3	X_4	X_5 (X_1X_3)	X_6 (X_1X_4)	% crystallinity	% yield
11	-	-	-	-	+	+	77.4	51.24
13	+	-	-	-	-	-	60	50.78
14	-	+	-	-	+	+	83.9	50.62
6	+	+	-	-	-	-	87	50.9
5	-	-	+	-	-	+	68.9	50.1
12	+	-	+	-	+	-	91.6	52.5
9	-	+	+	-	-	+	77.8	48.6
10	+	+	+	-	+	-	65.20	51.6
16	-	-	-	+	+	-	77.63	50.84
8	+	-	-	+	-	+	48.5	51.07
4	-	+	-	+	+	-	71.76	49.6
7	+	+	-	+	-	+	57.02	49.9
2	-	-	+	+	-	-	57.5	50.08
3	+	-	+	+	+	+	82.1	51.3
15	-	+	+	+	-	-	47.9	50.5
1	+	+	+	+	+	+	82.47	47.6
Repeat Trials								
17	+	+	+	-	+	-	71.32	51.43
18	+	+	+	-	+	-	60.19	51.74
19	+	+	+	-	+	-	86.5	51.22

where \underline{X} is the design matrix. \underline{X}^T is the transpose of the design matrix, \underline{Y} is the vector responses and $\hat{\underline{b}}$ is the vector of coefficients. The details of the method are given by Draper and Smith [22]. This is then tested for model adequacy by a Lack-of-fit F test. With the experimental results are given in Table 4.2, the fitted first order models for % crystallinity, % yield are given below by equations (4.1.5) and (4.1.6).

$$\begin{aligned}\hat{Y}_c = & 71.04 + 0.70x_1 + 0.58x_2 + 0.64x_3 - 5.43x_4 \\ & + 7.96x_5 + 9.36x_6\end{aligned}\quad (4.1.5)$$

$$\begin{aligned}\hat{Y}_y = & 50.45 + 0.25x_1 - 0.537x_2 - 0.16x_3 - 0.34x_4 \\ & + 0.21x_5 - 0.39x_6\end{aligned}\quad (4.1.6)$$

where \hat{Y}_c , \hat{Y}_y represent the predicted values of % crystallinity, % yield respectively. The lack of fit F tests for the above models are shown in Tables 4.3 and 4.4 respectively. A model calculation of the analysis of variance

(ANOVA) needed for conducting the lack-of-fit F-test is shown in Appendix.

It is observed from Table 4.4 that a simple first-order model is not adequate for describe the % yield data. Hence a higher order model incorporating cross-product terms have been proposed and tested for lack-of-fit F-test. This is given in Tabel 4.5.

Table 4.3 First Order Response Surface Strategy (First Move)
1 Test for the Adequacy of the Model for % crystallinity

Model : $\hat{Y}_c = 71.04 + 0.700 x_1 + 0.58 x_2 + 0.64 x_3 - 5.43 x_4$
 $+ 7.96 x_5 + 9.36 x_6$

ANOVA

Source	Sum of squares	Degrees of freedom	Mean square
Residual	4161.25	12	
Pure error	390.69	3	130.23
Lack-of-fit	3770.55	9	418.95

$$F_{cal} = \frac{418.95}{130.23} = 3.22$$

$$F_{0.05(9,3)} = 8.81$$

Model is adequate

Table 4.4 First Order Response Surface Strategy (First Move) Test for the Adequacy of the Model for % yield

Model : $\hat{Y}_c = 50.45 + 0.25 x_1 - 0.53 x_2 - 0.16 x_3 - 0.34 x_4$
 $+ 0.21 x_5 - 0.39 x_6$

ANOVA

Source	Sum of squares	Degrees of freedom	Mean square
Residual	10.00		
Pure error	0.15	3	0.05
Lack-of-fit	9.85	9	1.09

$$F_{cal} = \frac{1.09}{0.05} = 21.77$$

$$F_{0.05(9,3)} = 8.81$$

Model is not adequate

114318

The cross product terms which have influence on yield are given below with the values of the coefficients

$$\hat{b}_{12} = -0.17, \quad \hat{b}_{23} = -0.173, \quad \hat{b}_{24} = -0.174$$

$$\hat{b}_{25} = -0.27, \quad \hat{b}_{34} = -0.07, \quad \hat{b}_{36} = -0.48$$

$$\hat{b}_{26} = -0.34$$

out of the above seven terms we have neglected the terms \hat{b}_{12} and \hat{b}_{34} because of their relatively smaller values. Hence a better model can be proposed incorporating the remaining five terms with the first-order model, the model then takes the following form,

$$\begin{aligned} Y = & 50.45 + 0.25 x_1 - 0.54 x_2 - 0.17 x_3 \\ & - 0.34 x_4 + 0.21 x_5 - 0.39 x_6 - 0.173 x_2 x_3 - 0.174 x_2 x_4 \\ & - 0.27 x_2 x_5 - 0.34 x_2 x_6 - 0.48 \end{aligned}$$

Table 4.5 First Order Response Surface Strategy (Second Move):
Test for the Adequacy of the Model for % yield

Model : $Y = 50.45 + 0.25 x_1 - 0.54 x_2 - 0.17 x_3 - 0.34 x_4$
 $+ 0.21 x_5 - 0.39 x_6 - 0.173 x_2 x_3 - 0.17 x_2 x_4$
 $- 0.27 x_2 x_5 - 0.34 x_2 x_6 - 0.48 x_3 x_6 \quad (4.1.7)$

ANOVA

Source	Sum of squares	Degrees of freedom	Mean square
Residual	1.78		
Pure error	0.15	3	0.05
Lack-of-fit	1.63	9	0.18

$$F_{cal} = \frac{0.18}{0.05} = 3.6$$

$$F_{0.05(9,3)} = 8.81$$

Model is adequate

The effect of different variables on responses is evident from the values of coefficients of the corresponding model. The magnitude of the coefficient represents the amount of change in the response for the change of variable from the base level to the upper level. Negative sign of the coefficient indicates the same but in the opposite sense.

4.1.2.4 CALCULATION OF THE PATH OF STEEPEST ASCENT AND CONDUCT OF EXPERIMENT ALONG THIS PATH

Information obtained from the models was used to locate the path of maximum increase in crystallinity. The method of steepest ascent is a procedure for moving sequentially along the direction of maximum increase in response.

The direction of steepest ascent was determined using the relation.

$$\nabla\phi = \frac{\delta\phi}{\delta x_1} \vec{u}_1 + \frac{\delta\phi}{\delta x_2} \vec{u}_2 + \dots + \frac{\delta\phi}{\delta x_k} \vec{u}_k \quad (4.1.7)$$

where,

ϕ is the function describing the response surface,

$\nabla\phi$ is the gradient of the response function,

$\frac{\delta\phi}{\delta x_i}$ is the partial derivative of the function with respect to the i -th factor,

and $\vec{u}_1, \vec{u}_2 \dots \vec{u}_k$ are the unit vectors in the direction of the coordinate axes

It can be easily verified that the components of the gradient $\nabla\phi$ i.e. $\frac{\delta\phi}{\delta x_i} (i=1,2,\dots,k)$ are the same as the regression coefficients in Equation (4.1.3). Thus by changing the independent variables X_1 to X_6 in proportion to the values of their corresponding coefficients, the movement along the steepest path may be realised. From the coefficient of the fitted model for crystallinity (Equation 4.1.5) it is easy to compute these factor level. Combination which predict an increase in the % crystallinity of zeolite A. The calculation of this path is shown in Tabel 4.6. The details of these calculation are described below :

First two rows of the table indicate the values of the base levels and variation intervals of different factors. In the third row the regression coefficients of the model are given. These coefficients represents the gradient of the crystallinity in their respective directions. The fourth row was obtained by multiplying the unit of each factor with its coefficient so as to change the factor level in proportion to its slope (i'e., its regression coefficient). In the fifth row step changes in the factors X_6 and X_1 to x_4 were

calculated corresponding to a change of 5°C in the direction of factor x_5 . The choice of the size of the step change in factor x_5 is a matter of experimental convenience. The fifth row was then added (element by element) to the original base levels in the first row to get the elements of the first trial point in the path of the steepest ascent. The second trial point in the path is obtained by adding the first point to the elements of fifth row. This process is then iterated to get the other points of the path. Additional experiments were then performed (runs numbered 20,21,22,23) according to trial points 1 to 4. The experimental results and values predicted by the first order model (Equation 4.1.5) are given in Table 4.7.

From Table 4.7 it is observed that a maximum crystallinity of 92.05% can be achieved under the following condition :

$$\frac{\text{SiO}_2}{\text{Al}_2\text{O}_3} \text{ (mole) Ratio } (x_1) = 1.31$$

$$\frac{\text{Na}_2\text{O}}{\text{SiO}_2} \text{ (mole) Ratio } (x_2) = 3.61$$

$$\text{pH } (x_3) = 13.62$$

$$\text{Temperature of hydrogel formation } (x_4) = 35.76^{\circ}\text{C}$$

$$\text{Temperature of crystallization } (x_5) = 110^{\circ}\text{C}$$

$$\text{Reaction time } (x_6) = 51 \text{ hours}$$

Table 4.6 First Order Response Surface Strategy (First Move) :
Calculation of the path of Steepest Ascent

	FACTOR					
	x_1	x_2	x_3	x_4	x_5	x_6
Base Level :	1.25	3.45	13.5	37.5	95	30
Unit :	0.5	1.5	1	5	10	12
Estimated Slope :	0.70	0.58	0.64	-5.43	7.96	9.36
Unitxb:	0.35	0.87	0.64	-27.15	79.63	112.33
Charge in level per 5°C change in x_5	0.02	0.05	0.04	-1.70	5	7.05
Path of Steepest Ascent as Represented by a Series of Trial points						
Trial Point	x_1	x_2	x_3	x_4	x_5	x_6
1	1.27	3.50	13.54	39.20	100	37.05
2	1.29	3.55	13.58	37.46	105	44.1
3	1.31	3.61	13.62	35.76	110	51.15
4	1.38	3.82	13.74	34.54	115	58.2

Table 4.7 First Order Response Surface Strategy (First Move) : Results of Experiments along the path of Steepest Ascent :

Run No.	Trial point	Experimental % crystallinity	Predicted %
20	1	89.64	90.24
21	2	91.3	91.7
22	3	92.05	92.01
23	4	90.6	90.31

Effect of operating variables

The details for the different runs conducted with the composition, time of reaction and the temperature as variable together with percentage crystallinity and percentage yield of zeolite A are indicated in Tabel 4.2.

The effect of important variables against % crystallinity and % yield is also shown in Figure 4.1 to Figure 4.3. The initial composition of the mixture is paramount importance in governing the type of crystallized zeolite and the percentage crystallization of zeolite A.

Silica and Alumina Molar Ratio $\left(\frac{\text{SiO}_2}{\text{Al}_2\text{O}_3} \right)$

It has been observed that the percentage crystallization and yield of zeolite A increases with the silica content in the starting gel (Fig. 4.1). This is possible due to the formation of more sodalite units which in turn join to produce zeolite Na-A.

The increase in the yield with increasing Silica content of the mixture is in conformity with the findings of the earlier workers (33).

Reaction temperature

The effect of reaction temperature on the percentage crystallization and yield is indicated in Fig. 4.2.

The increase in percentage crystallinity and yield of zeolite A with temperature observed in the present work is in accordance with the earlier reported by Cho et al. (34).

Reaction time

The crystallization and yield curves for zeolite A at different times are indicated in Fig. 4.3. The crystallinity curve exhibits a characteristic shape denoting rapid crystallization with time.

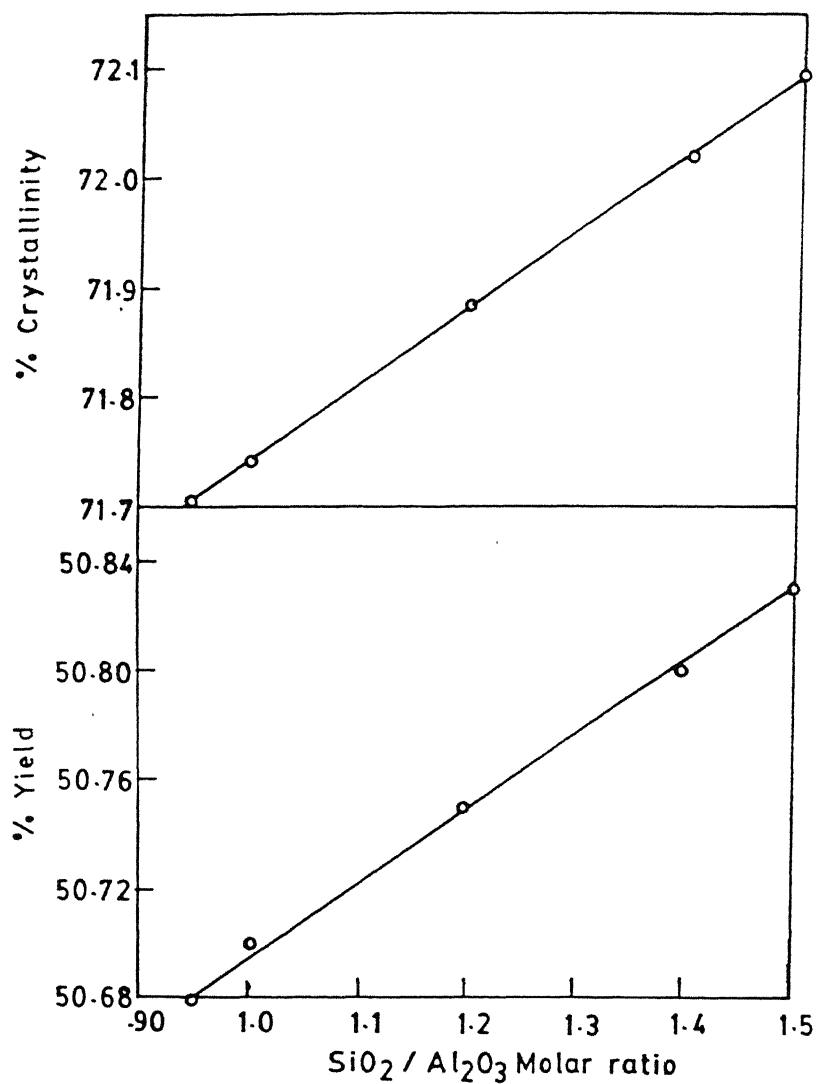


FIG. 4-1 EFFECT OF SILICA ALUMINA RATIO ON ZEOLITE A CRYSTALLIZATION AND YIELD AT 95 °C FOR 30 Hrs.
 $\text{H}_2\text{O} / \text{Al}_2\text{O}_3 = 210$

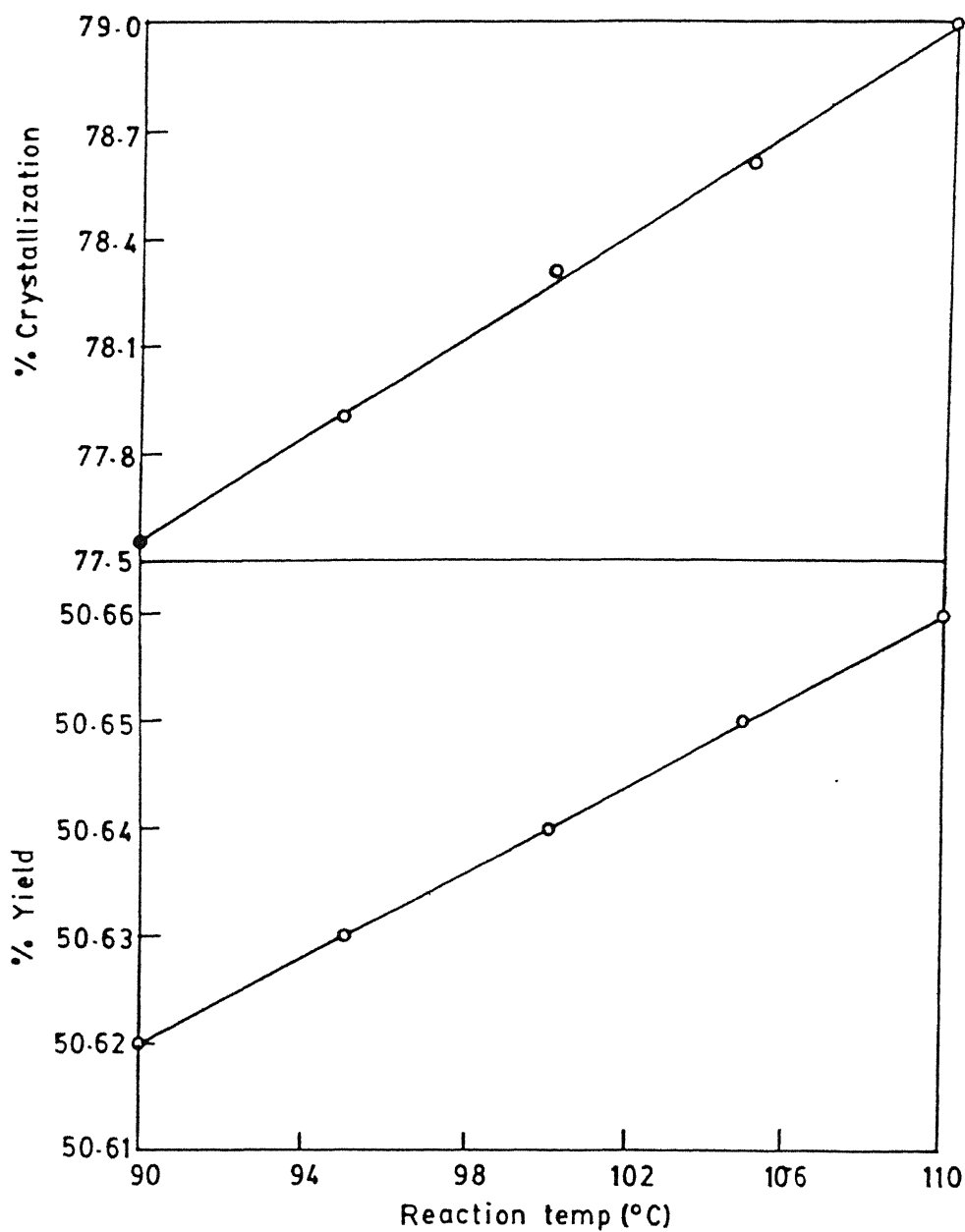


FIG. 4-2 EFFECT OF REACTION TEMPERATURE ON ZEOLITE A
CRYSTALLIZATION AND YIELD AT $\text{SiO}_2/\text{Al}_2\text{O}_3$ (Molar)
RATIO 1-25 FOR 30 Hrs. $\text{H}_2\text{O}/\text{Al}_2\text{O}_3=210$

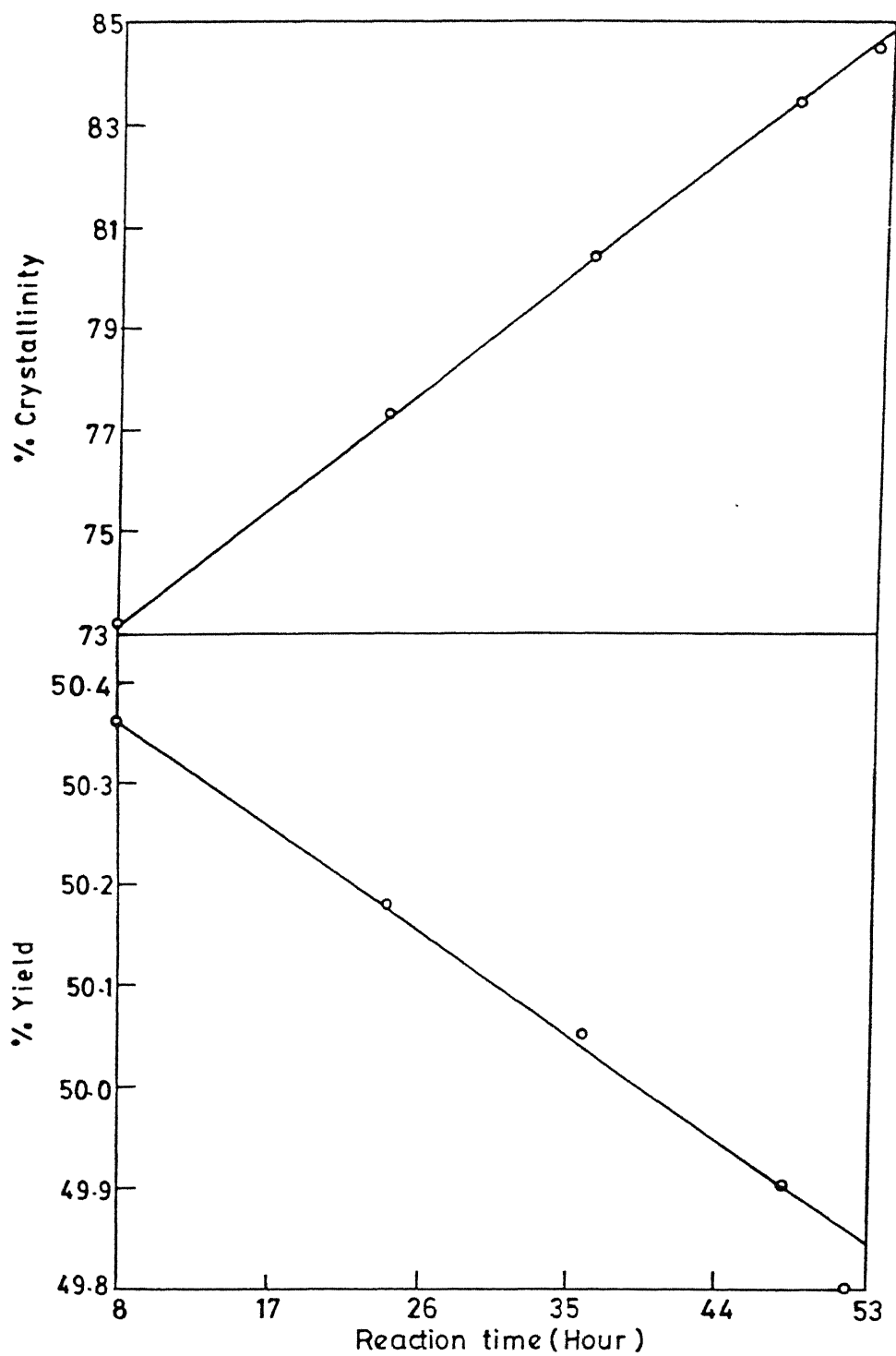


FIG. 4.3 EFFECT OF REACTION TIME ON ZEOLITE A CRYSTALLIZATION AND YIELD AT 95 °C FOR $\text{SiO}_2 / \text{Al}_2\text{O}_3$ (Molar) RATIO 1.25 AND $\text{H}_2\text{O} / \text{Al}_2\text{O}_3 = 210$

But yield curve shows reverse characteristics. The yield of Na-A zeolite reduces with time. This may be due to the dissolution of gel materials and the formation of Al(OH)_n , when solution of aluminate and Silicate or polysilicte anions are mixed to form the hydrogels.

4.3 CHARACTERIZATION OF ZEOLITE Na-A

In the present study, the zeolite Na-A obtained from starting material using silica and alumina from diatomaceous clay has been studied using several techniques for its characterization.

4.3.1 X-RAY DIFFRACTION DATA

Figure 4.4 shows the X-ray pattern of calcined diatomite. It is seen that the peaks are very broad. The peak broadening is due to the fine particle size of diatomite. This implies that the diatomite used here is quite reactive.

Table 4.8 gives the standard data for zeolite A from two literature sources while Table 4.9 and Table 4.10 gives the literature data for zeolite P_c and zeolite H_s respectively. Figure 4.5 give the diffractogram for zeolite Na-A (standard 4A molecular sieve).

The diffractograms obtained from eight of the samples are given in Figure 4.6 and 4.7. X-ray data for a typical sample is also included in Table 4.8. A comparison of Table 4.8 and Table 4.9 & 4.10 as well as Figure 4.5 and Figure 4.6 & 4.7 shows that the data matches very well with zeolite Na-A except for two small peaks at $2\theta = 14^\circ$ and $2\theta = 17.8$ degrees.

The peak at $2\theta = 14^\circ$ degrees corresponds to the 80% peak of zeolite HS (Table 4.10). The peak at $2\theta = 17.8$ degrees corresponds to the 35% peak of the zeolite P_c . This shows that the samples prepared by us are mostly zeolite A with small amount of zeolite HS and zeolite P_c .

In this study zeolite Na-A was synthesized from diatomite (calcined) as a source of silica and alumina. Maximum conversion of Na-A zeolite was obtained around 110°C with reaction time 52 hours.

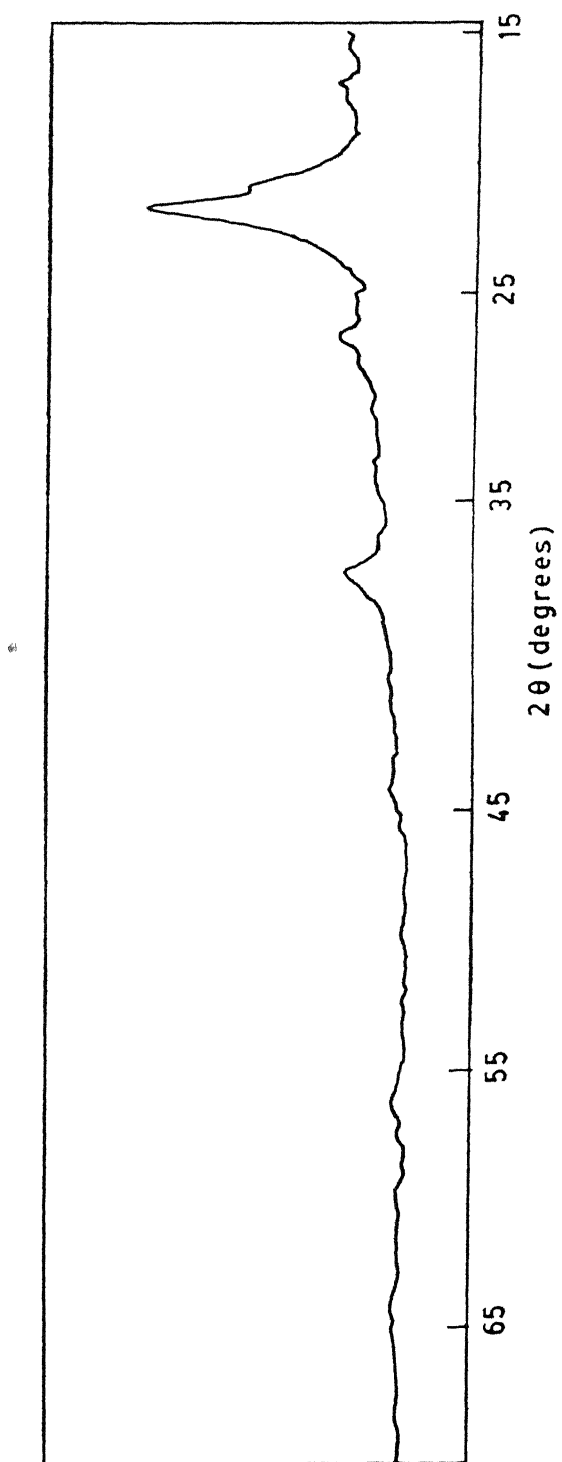


FIG.4.4 X-RAY PATTERN OF DIATOMACEOUS CLAY

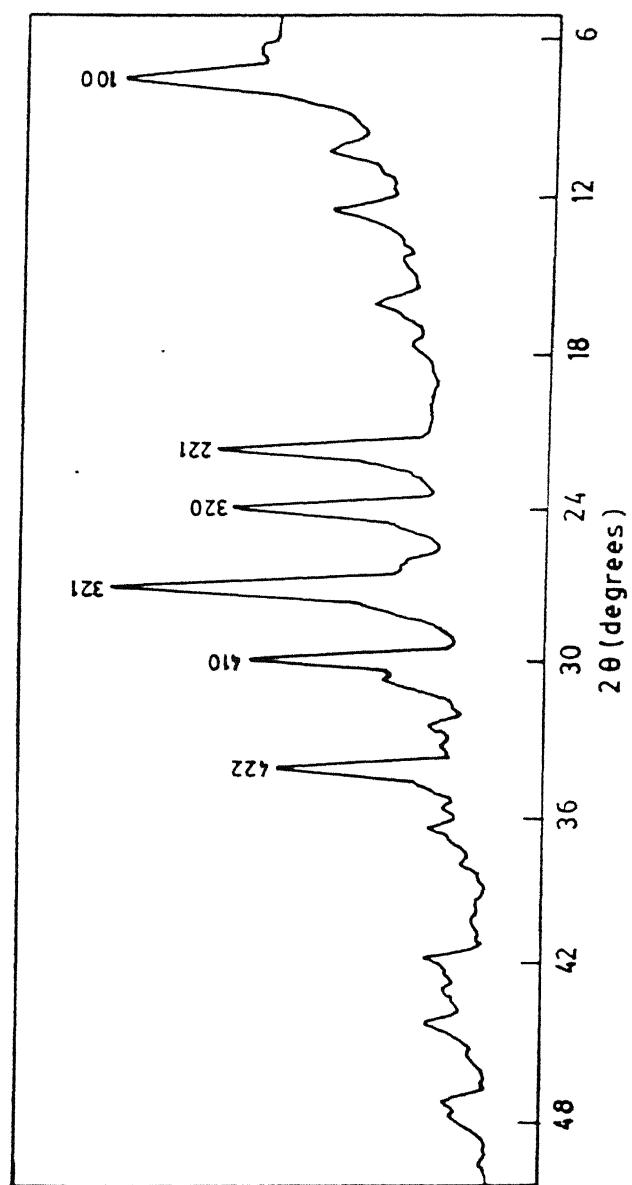


FIG. 4.5 X-RAY PATTERN OF STANDARD ZEOLITE 4A

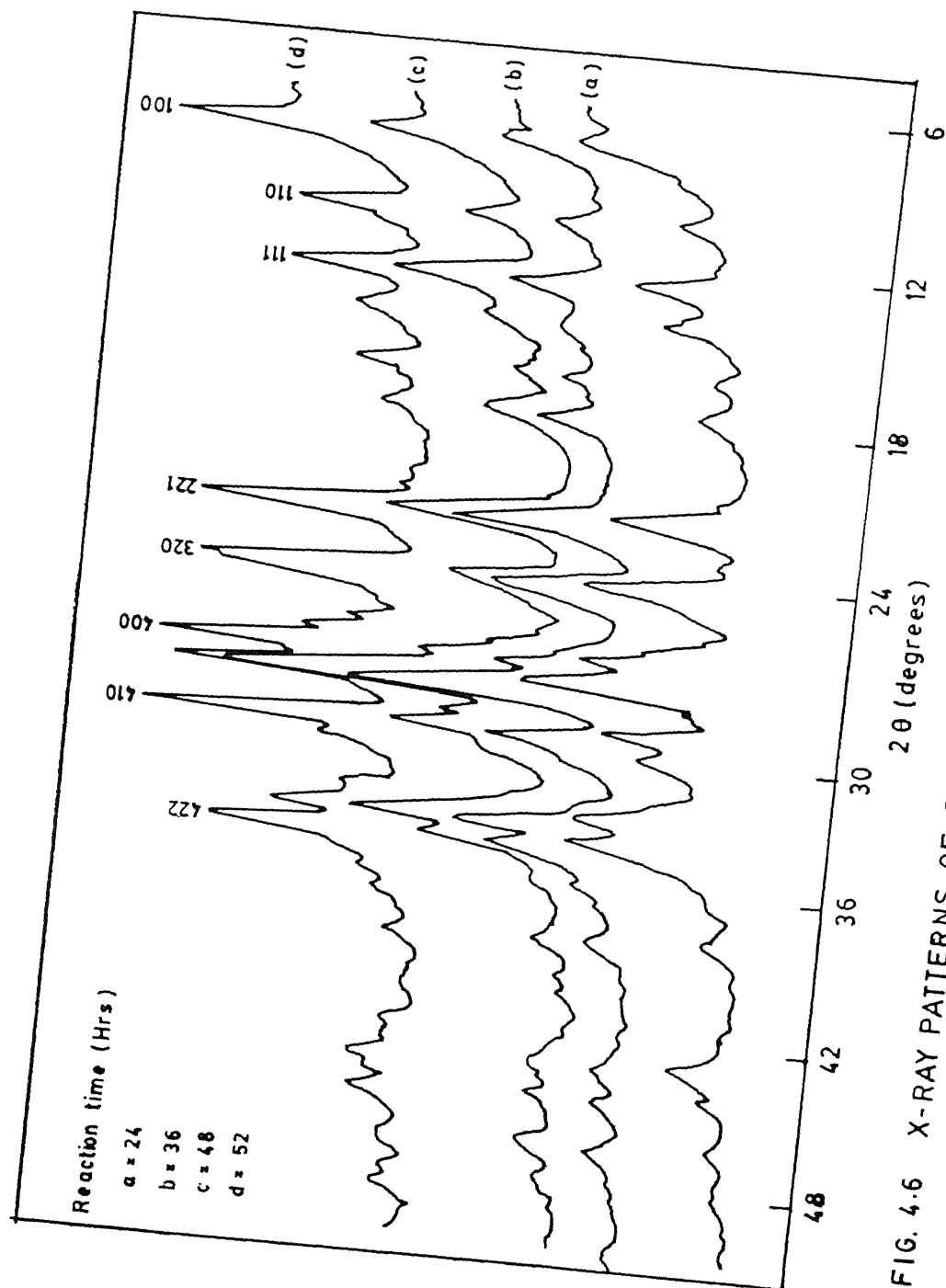


FIG. 4.6 X-RAY PATTERNS OF SYNTHESIZED ZEOLITE A

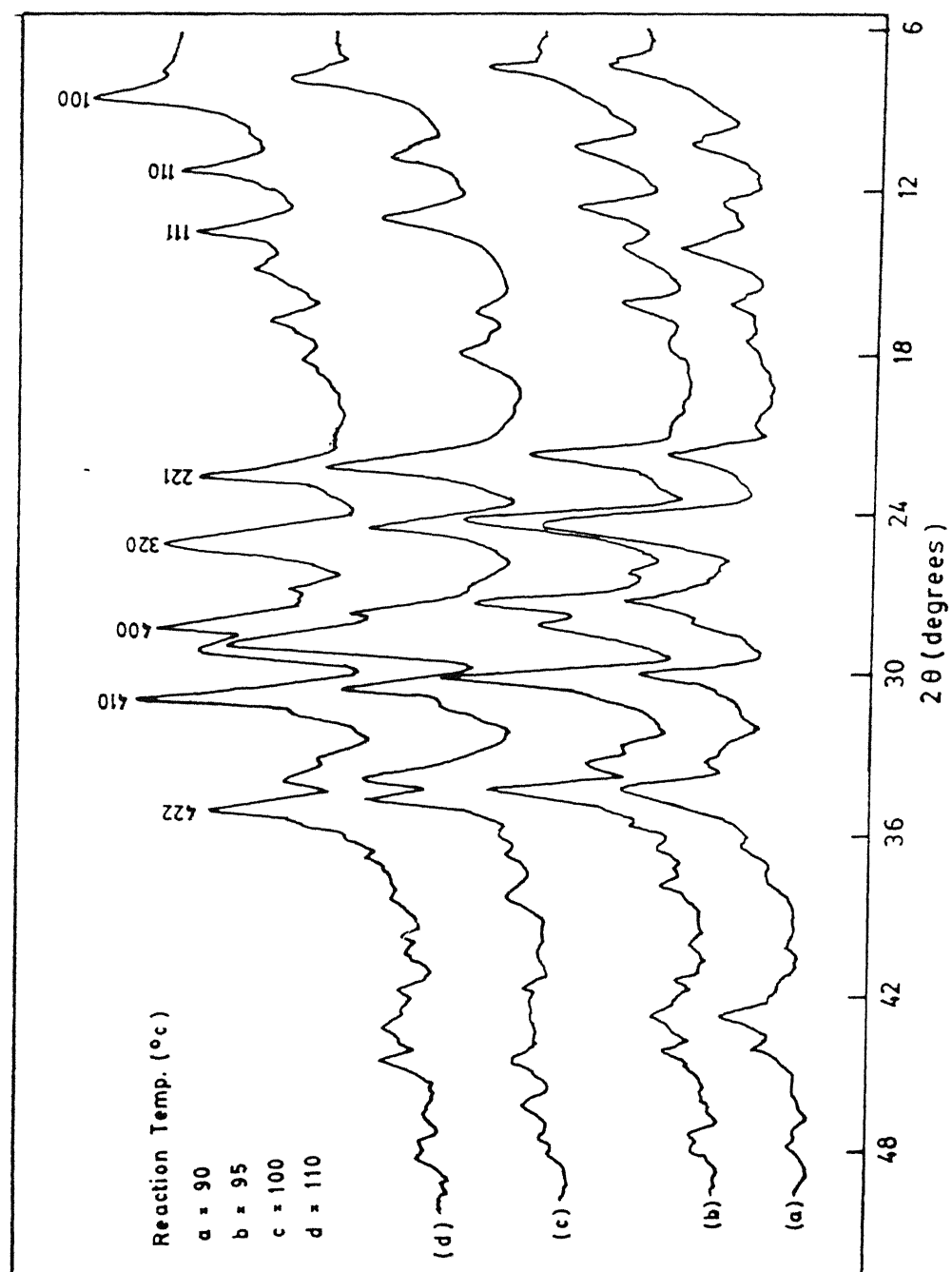


FIG. 4.7 X-RAY PATTERN OF SYNTHESIZED ZEOLITE A

Table 4.8 X-ray powder data for Zeolite Na-A

(hkl)	Literature value of Na-zeolite Ref(35)			Literature value of 4A Molecular Sieve			This study (Sample 10)		
	d(Å)	2θ	I/I ₀ ×100	d(Å)	2θ	I/I ₀ ×100	d(Å)	2θ	I/I ₀ ×10
100	12.3	7.28	69.9	12.3	7.28	69.9	12.3	7.2	35.5
110	8.5	10.3	67.9	8.5	10.3	67.9	8.6	10.3	26
111	7.1	12.5	33.1	7.1	12.5	33.1	7.1	12.6	54
200							6.3	14	6
210							49	17.8	29
221	4.1	21.9	60.2	4.1	21.9	60.2	4.1	21.8	69.3
320	3.6	24.3	100	3.6	24.3	100	3.7	24.2	100
321	3.2	27.3	23.3	3.2	27.3	23.3	3.1	27.1	89.3
400	3.04	28.2	81.5	3.04	28.2	81.5	3.2	28.2	33.3
410	2.9	30.1	94.2	2.9	30.1	94.2	2.9	30.2	62.5
422	2.6	34.4	62.2	2.6	34.4	62.2	2.6	34.3	51.8
430				2.5	35.9	5			
511				2.4	37.4	4			
520				2.3	39.1	1			
441				2.1	42.2	10			
600				2.05	44.2	9			

Table 4.9 X-ray Powder data for Zeolite P_c

2θ	$d(\text{\AA})$	(hkl)	$I/I_0 \times 10$
12.45	7.1	(110)	55
17.68	5.01	(200)	35
21.65	4.10	(211)	55
28.2	3.16	(310)	100
33.53	2.67	(321)	55
35.59	2.52	(400)	5
38.09	2.36	(411)	7
44.05	2.05	(422)	5
46.16	1.97	(510)	10
51.56	1.77	(440)	7
53.24	1.72	(530)	7
55.04	1.67	(600)	7

Table 4.10 X-ray Powder data for Zeolite HS :

2θ	$d(\text{\AA})$	(hkl)	$I/I_0 \%$
14.09	6.28	(110)	80
19.98	4.44	(200)	30
22.37	3.97	(210)	5
24.50	3.63	(211)	100
28.49	3.13	(220)	60
31.82	2.81	(310)	80
35.02	2.56	(222)	30
37.93	2.37	(321)	30
43.25	2.09	(330)	80
45.54	1.99	(420)	5
48.15	1.88	(332)	9
50.25	1.81	(422)	30
52.65	1.74	(501)	40
56.65	1.62	(521)	5
58.63	1.57	(440)	30
60.76	1.52	(530)	30

4.3.2 INFRARED SPECTROSCOPY

The infrared spectra of synthesized zeolites and standard Na-A zeolite (4A molecular sieve) are presented in Figure 4.8 and Figure 4.9 respectively. The infrared spectra of synthesized zeolites shows the absorption bands at 3450 (W), 1640 (Sh), 1000 (VS), 740 (m), 670 (m) cm^{-1} in the 4000 - 600 cm^{-1} range.

The spectra of standard 4A zeolite is shown in the Figure 4.9.

The spectra obtained from three samples are given in Figure 4.8. A comparison of Figure 4.8 and Figure 4.9 shows that the absorption bands match very well with zeolite Na-A except for one small absorption band at 1450 cm^{-1} which is assigned to the internal asymmetric stretching vibration. The medium weak absorption at 740 cm^{-1} and 670 cm^{-1} are attributed to the external symmetric stretching vibration. The three typical bands are also presented which characteristics of hydrogen bond (OH) at 3450 cm^{-1} and at 3500 cm^{-1} the isolated (OH) and usual bonding vibration of the water at 1640 cm^{-1} .

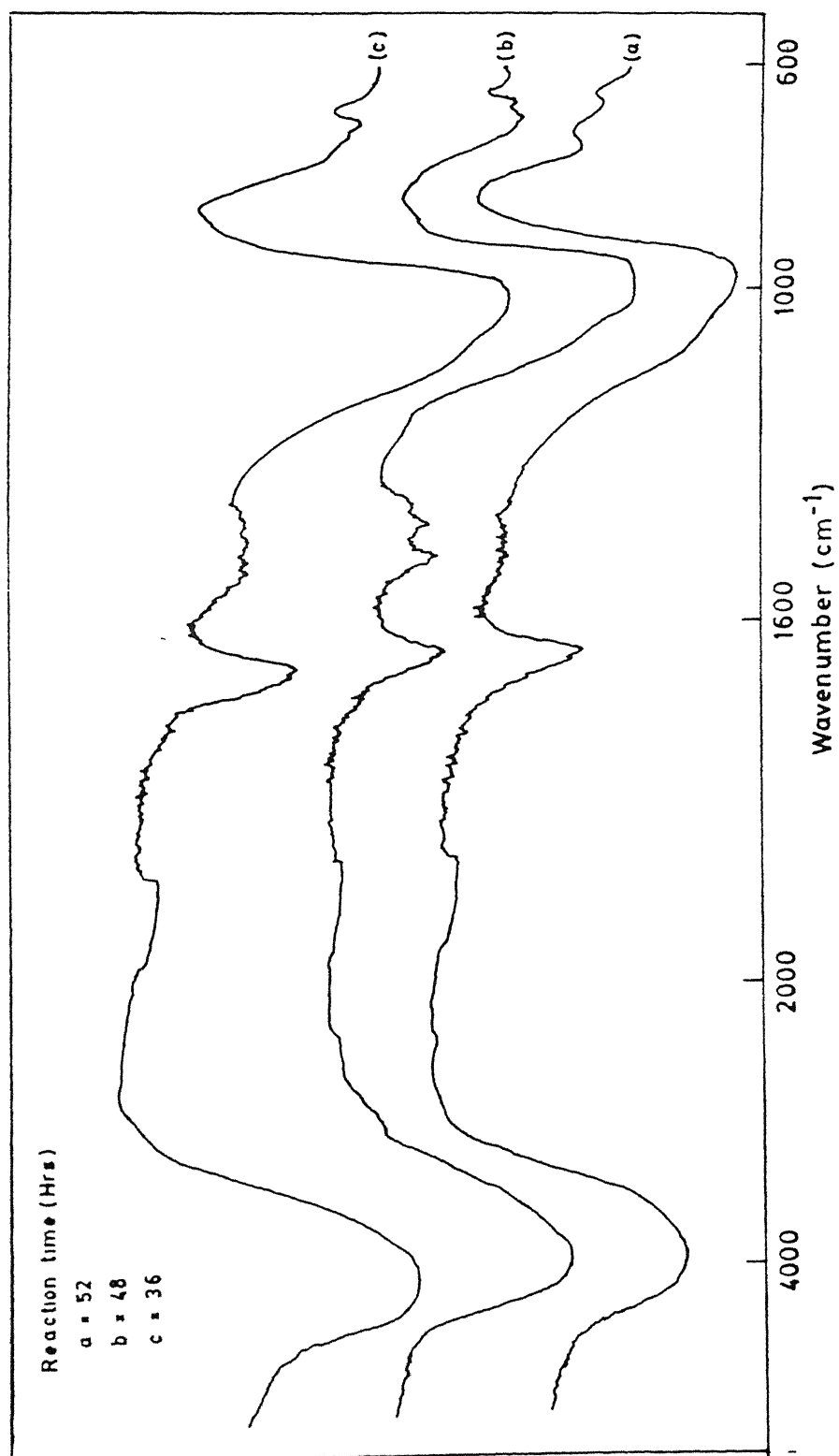


FIG. 4.8 INFRARED SPECTRA OF SYNTHESIZED ZEOLITES

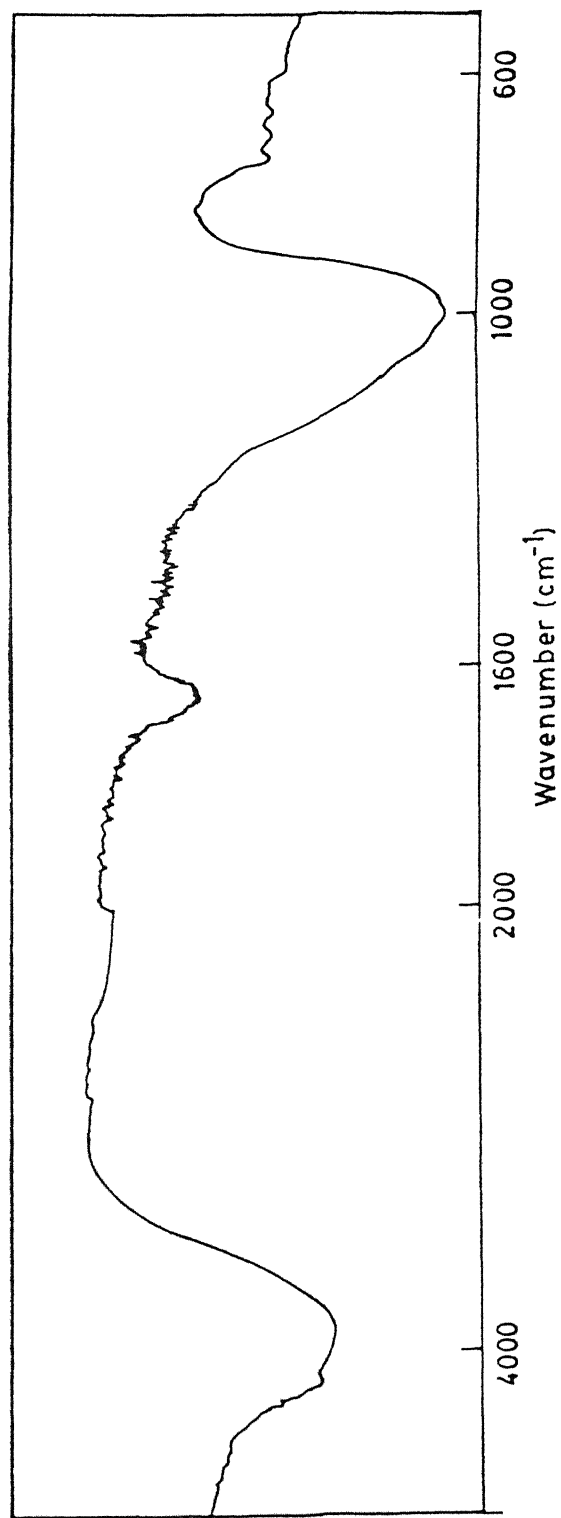


FIG. 4.9 INFRARED SPECTRA OF STANDARD (4A) ZEOLITE

4.3.3 PARTICLE SIZE ANALYSIS

Particle size analysis was done on three samples of synthesized zeolite powder. Figure 4.10 shows the average particle size distribution. The average particle size (50% cumulative probability) is given in Table 4.11.

Table 4.11 Particle Size Analysis by Coulter-Counter Method

Sample	Temp (Reaction)	Temp (Teaction)	Average Particle size (μm)
Run no. 14	90 ⁰ C	36 hours	5.125
Run no. 5	95 ⁰ C	36 hours	5.125
Run no. 22	110 ⁰ C	52 hours	3.5

4.3.4 SCANNING ELECTRON MICROSCOPY (SEM)

Figure 4.13(a) is a low magnification scanning electron micrograph of the sample prepared at 110⁰C (sample no. 22). Most of the particles are spherical in shape while a few have a cubic shape. It is known that the zeolite Na-A powder have mostly spherical morphology (36). On the other hand zeolite HS particles have mostly cubic shape. The X-ray data of our

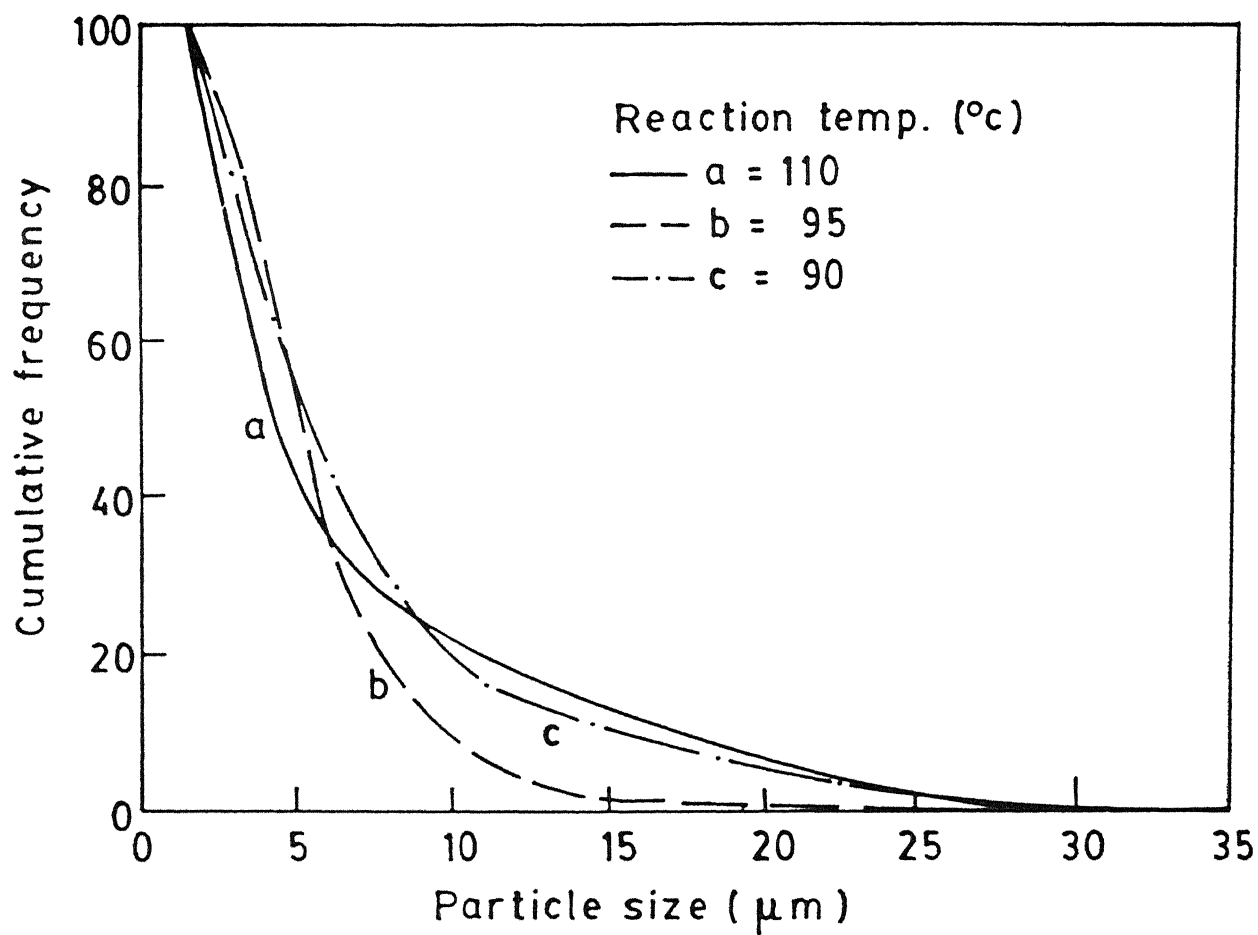


FIG. 4.10 PARTICLE SIZE ANALYSIS OF SYNTHESIZED ZEOLITE

samples shows that predominant phase is zeolite A; small amounts of zeolite HS also show up in the X-ray diffractogram. In view of this, it is reasonable to conclude that the spherical particles in Fig. 4.13 are of zeolite A and the cubic particles belong to the zeolite HS.

The largest particles observed in SEM are about 8 μm while the average size is 3-4 μm (Fig. 4.13(a)). The average size agrees well with the average size determined from the Coulter-Counter (Fig. 4.10). However the Coulter-Counter data indicates presence of particles as large as 30 μm as compared to 8 μm in the SEM. This seems to be due to agglomeration of the particles; while the aggregates are resolved in the SEM, they are not in the Coulter Counter.

Fig. 4.13(b) & 4.14(a) is a high magnification scanning electron micrograph of a spherical particle from sample 22. The particle consists of a network of needles of average length 0.4 μm and thickness 0.08 μm . This kind of structure is characteristic of zeolite A (36).

Fig. 4.14(b) shows a particle of zeolite HS (cubic) in high magnification. The surface is featureless; there are no pores or needles. The pore size is too small to be resolved by SEM.

4.3.5 BET SURFACE AREA MEASUREMENT

The values of surface areas are given in Table 4.12 along with the standard values for the zeolite A. The values obtained for the synthesized zeolites in this study are nearly equal to the standard zeolite A. The values are somewhat lower than the standard Na-A zeolite (standard 4A zeolite).

Table 4.12 Surface Areas of Synthesized Zeolite A

Zeolites	Surface Area m^2/gm
Standard 4A Zeolite	28
Synthesized Zeolite A $\left[\frac{\text{SiO}_2}{\text{Al}_2\text{O}_3} \text{ molar ratio} = 1.5 \right]$	23.1
Synthesized Zeolite A $\left[\frac{\text{SiO}_2}{\text{Al}_2\text{O}_3} \text{ molar ratio} = 1 \right]$	26.8
Synthesized Zeolite A $\left[\frac{\text{SiO}_2}{\text{Al}_2\text{O}_3} \text{ molar ratio} = 0.95 \right]$	27.2

Ion Exchange

Calcium ion exchange capacity of synthesized zeolite Na-A is 5.4 meq/g.

Result of small-scale column tests are summarised in Fig. 4.11 & 4.12. The composition of feeding water was Ca^{+2} 165.20 mg/litre. In Fig. 4.11 a calcium break through curve, obtained under the conditions of 14 cm^3 bed volume, 3.5 μm particle size. 10 cc/min flow rate is shown. Calcium exchange capacity at saturation was 16.8 meq Ca^{+2} /g. Breakthrough of 25%, corresponding to Ca^{+2} CEC (cation exchange capacity) value required about 2.4 litre solution.

In the Fig. 4.12 is shown that the calcium and magnesium breakthrough occurs at lower volume 1.4 litre in the same experimental condition.

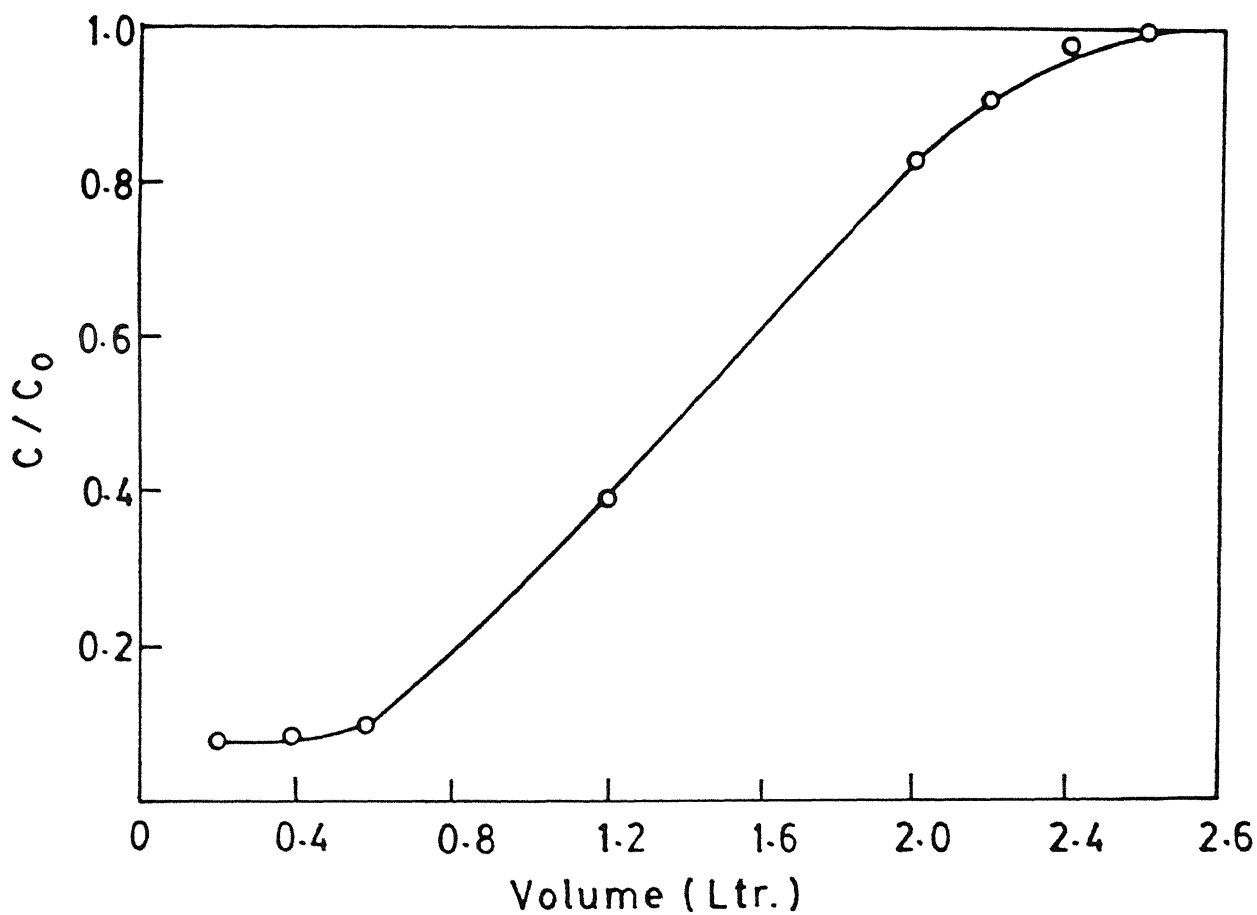


FIG. 4.11 CALCIUM BREAKTHROUGH CURVES FROM ZEOLITE A
 C_0 = INITIAL INLET CALCIUM CONCENTRATION

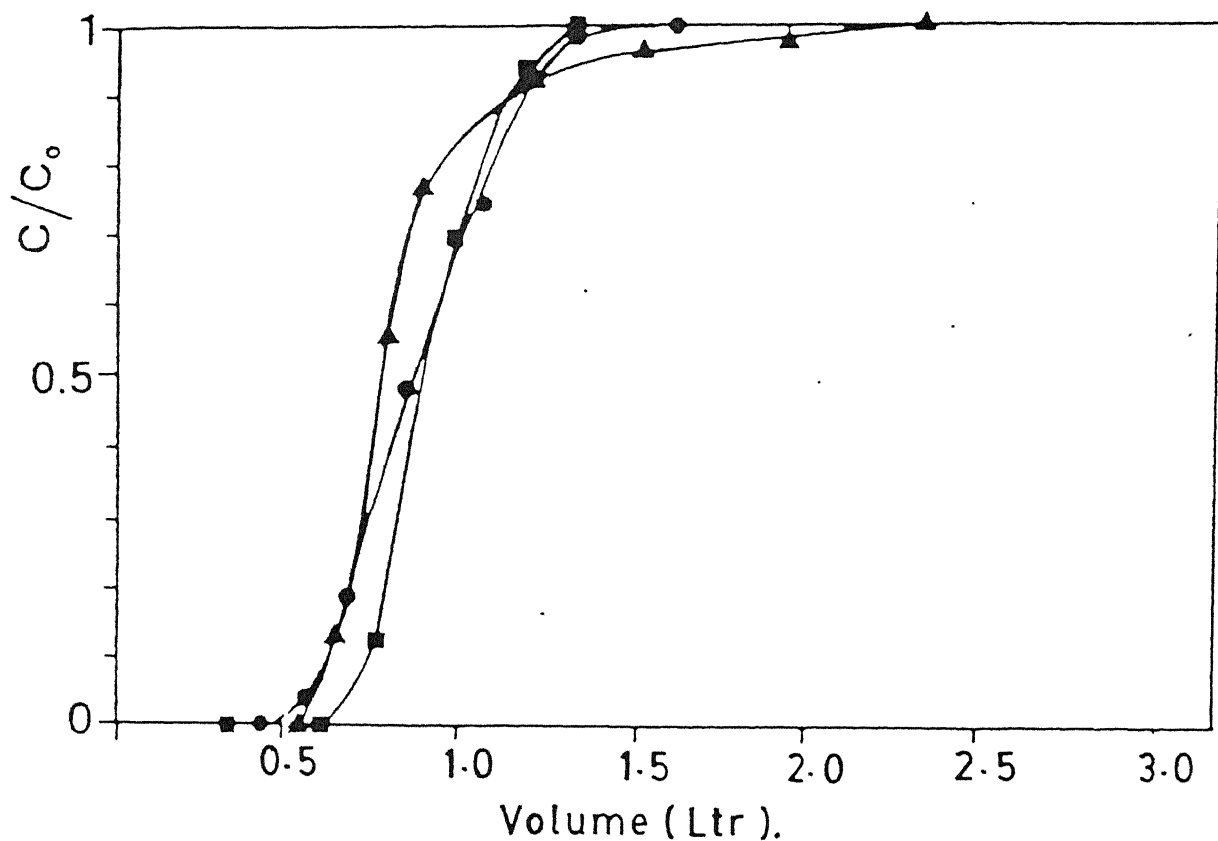


FIG.4.12 CALCIUM AND MAGNESIUM BREAKTHROUGH CURVES FROM ZEOLITE A .

(C_0 = Initial inlet Calcium and Magnesium concentration , Bed volume = 14 cm³ (●) ; 29 cm³ (▲) ; 14 cm³ (■) , Flow rate = 10 cc /min (●) ; 10 cc /min (▲) ; 5 cc /min (■) ,

CHAPTER-5

CONCLUSIONS AND RECOMMENDATIONS

In the present work diatomite was calcined at 900°C for 4 hours to undergo dehydroxylation. The process involves expulsion of (OH) from the clay structure. On calcination diatomite structure becomes cellular and is in an active form. It is more reactive compared to uncalcined diatomite because of its disordered state. The calcined diatomite was treated with 1:1 HCl to remove iron present in it. To the calcined diatomite, aluminium hydroxide was added to make up the total requirement of alumina in a batch.

Synthesis of zeolite A has been attempted in the temperature range of $90-110^{\circ}\text{C}$ with reaction time varying from 8-52 hours. The molar ratio of $\frac{\text{SiO}_2}{\text{Al}_2\text{O}_3}$ and $\frac{\text{Na}_2\text{O}}{\text{SiO}_2}$ have been varied in the ranges 1-1.5 and 2.5-4.4 respectively.

Optimum value of different variables like $\frac{\text{SiO}_2}{\text{Al}_2\text{O}_3}$ molar ratio, $\frac{\text{Na}_2\text{O}}{\text{SiO}_2}$ molar ratio of reaction mixture, temperature and time of reaction are obtained using fractional factorial design along with path of steepest calculation.

X-ray diffraction analysis of the products obtained from the runs conducted between 90°C-110°C have indicated gradual increase in the intensities of the characteristic peaks of zeolite A with increase in temperature, indicating the improvement in the amount of this product. Ratio of $\frac{\text{SiO}_2}{\text{Al}_2\text{O}_3}$ in the mix has been found to control the product formation.

Scanning electron microscopy has enabled the identification of the individual reaction-product at different stages in terms of their characteristic morphology. Zeolite A exhibits a characteristic polyhedral equidimensional crystal form. The forms exhibited by zeolites P_c and HS are distinctly different. Crystallite size varies from 1.4 to 5.5 μm.

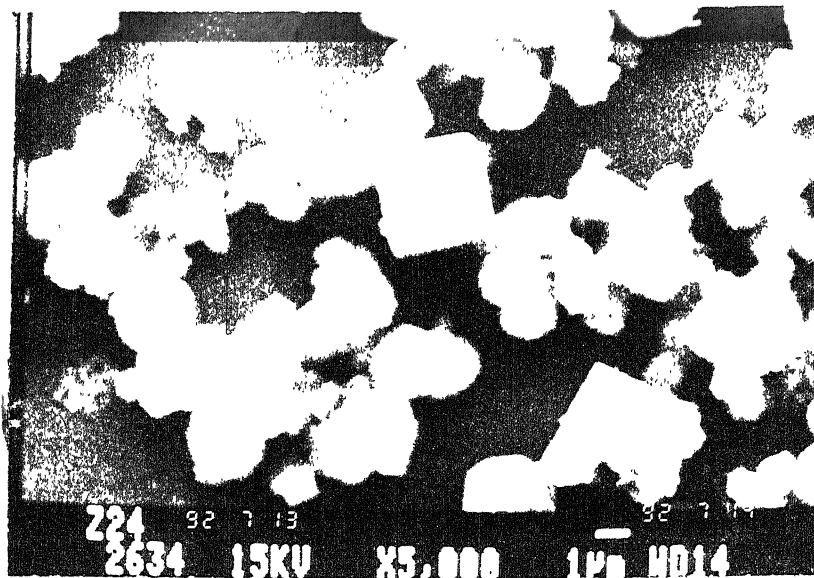
The product obtained at 100°C on complete conversion was characterized for its practical utility. In the present work synthesized zeolite was characterized for its use as ion exchanger in detergent builder component.

It has been found that using zeolite A a maximum ion exchange capacity is 5.4 meq/gm (calcium ion exchange capacity).

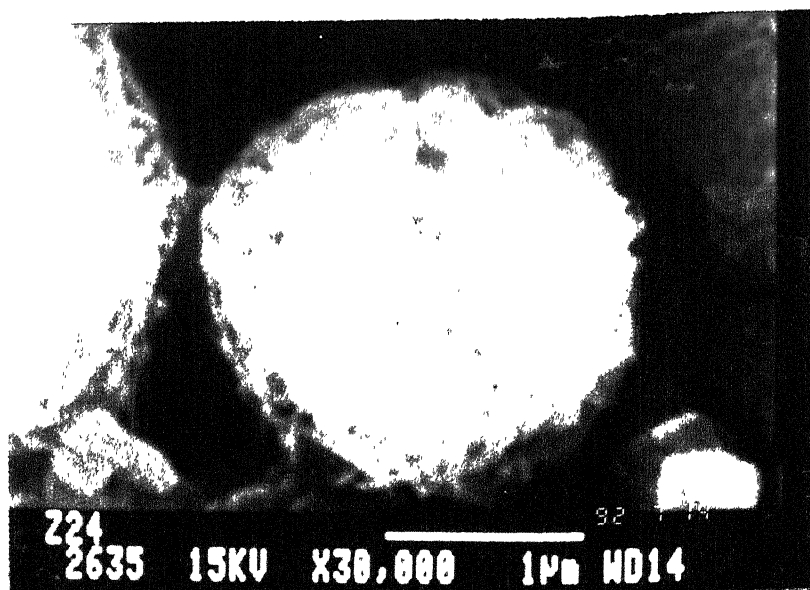
Recommendations

On the basis of the present study, the following recommendations are made for the future work :

1. The synthesis of zeolite A using other clay minerals such as Kaolinite, Montmorilloinite, Rice-husk ash sources of Silica and alumina should be tried.
2. Rapid synthesis of zeolite A by seeding with pure crystals of zeolite A should be attempted.
3. Other types of zeolite such as X, Y, mordenite & ZSM5 should also be synthesized using diatomaceous clay as a source of silica and alumina.
4. Adsorption & separation of gases, detergent builder characteristics should be attempted.

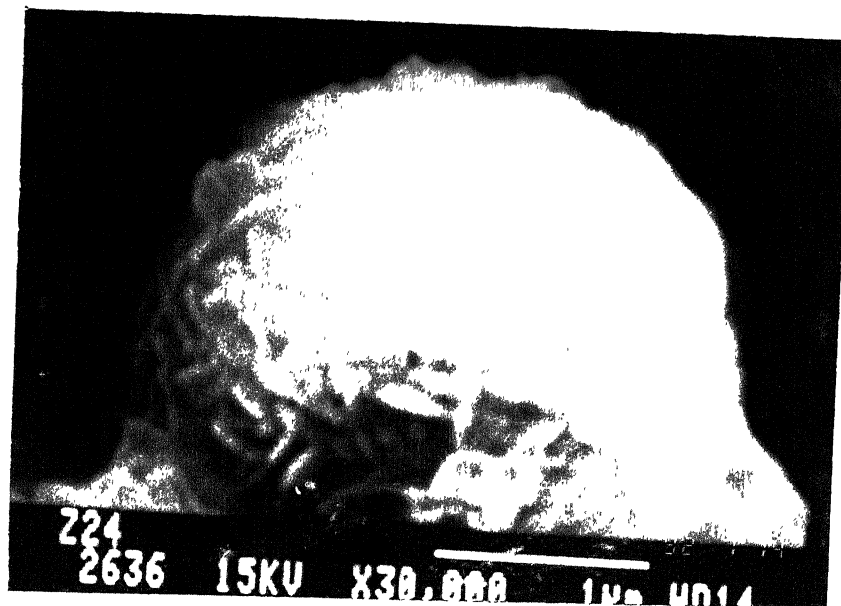


(a)

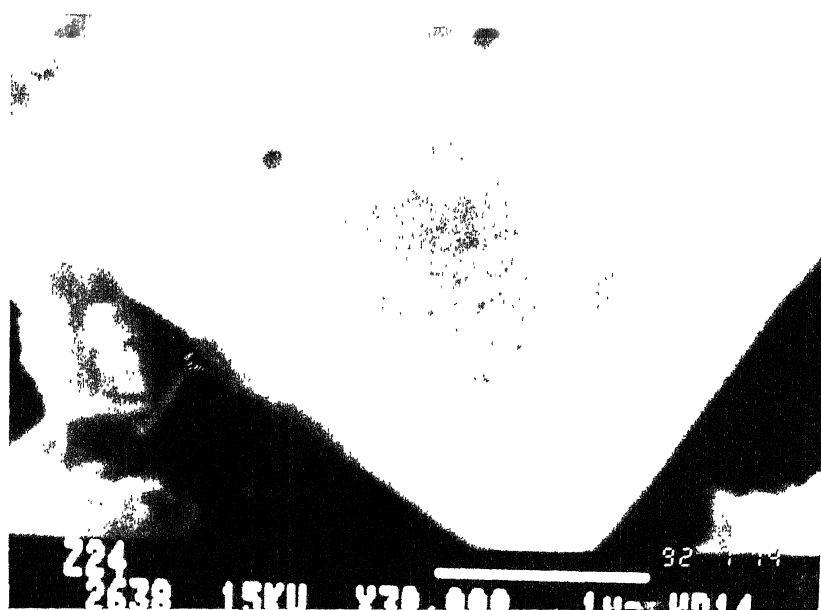


(b)

4.13 - SEM PHOTOGRAPHS OF SYNTHESIZED ZEOLITE



(a)



(b)

4.14 - HIGH MAGNIFICATION SEM PHOTOGRAPH OF SYNTHESIZED ZEOLITE

REFERENCES

1. Hersh, C.K., "Molecular Sieves", London (1964).
2. Bragg, L., Charingbull, G.F., "The Crystalline State, Crystal Structure of Minerals", Vol. IV, Cornell Univ. Press, Ithaca (1965).
3. Kuhl, G.H., "High-Silica Analogs of Zeolite A Containing Intercaalated phosphate", Inorganic Chemistry, 10 pp 2488 (1971).
4. Bhatia, S., "Zeolite Catalysis : Principle and application", CRC Press, (1990).
5. Scott, J., "Zeolite Technology and Application, Recent advances", Chemical Technology review No. 170.
6. Goldsmith, J., "A Simplexity Principle and its relation to ease of Crystallization", Jl. Geology, 61 439 (1953).
7. Fyfe, W.F., "Hydrothermal Synthesis and Determination of Equilibrium Between Minerals in the Subliquid Region", J. Geology, 68 : 553 (1960).
8. Jarman, R.H., "Application of Powder X-ray Diffraction Data to the Determination of frame-work Composition in Zeolites", Zeolites 5 : 213 (1981).
9. Flanigen, E.M., Khalami, H., Szymamki, H.A., "Infrared Structural Studies of Zeolite Frameworks", Adv. Chem Ser 101: 201 (1971).
10. Gogolyuk, S.A. Novosad, P.V., "Identification of Sodalite type mineral by IR Spectroscopy", USSR Vestn. L' VOV Politekh Inst. 201 : 5(1980) (as cited in chemical Abstracts 108 : 40305 d).
11. Industrial Eng. Chem. Res., Vol. 30, No. 8, Page (1675-1683), 1991.

12. Zhdanov, S.P., "Some Problems of Zeolite Crystallization", Adv. Chem. Ser. 101 : 20(1971).
13. Bertsch, L., Habgood, H.W., "An infrared Spectroscopic Study of the Adsorption of Water and Carbon Dioxide by Linde Molecular Sieve X", J. Phys. Chem. 67 : 1621 (1963).
14. Kittrell, J.R., Erjavec, J., Response Surface Methods in Heterogeneous Kinetic Modelling, Ind. Eng. Chem. Proc. Des. Dev., 1966, 7(3), 321-327.
15. Box, G.E.P., Hunter, W.G., Hunter, J.S., Statistics for Experiments., John Wiley & Sons: New York, 1978, Chapters 10 and 12.
16. Davies, D.L.; The Design and Analysis of Industrial Experiments; Longman Group Limited: New York, 1978; Chapter 11.
17. Khuri, A.I., Cornell, J.A., Response Surfaces Designs and Analysis., Marcel Dekker, Inc. : New York, 1987, Chapters 1,2,3 and 5.
18. Adler, Yu. P., Markova, E.V., Granovsky, Yu. V. The Design of Experiments to Find Optimal Conditions; Mir Publishers : Moscow, 1975.
19. Cochran, W.G., Cox, G.M., Experimental Designs, (2nd ed.), John Wiley & Sons: New York, 1957.
20. Hill, W.J., Hunter, W.G., A Review of Response Surface Methodology : A Literature Survey, Technometrics, 1966, 8(4), 571-590.
21. Rao, M.S., Iyengar, S.S. in Computer Modelling of Complex Biological System., (Eds. S.S.Iyengar) CRC Press, Inc., Boca Raton, Fla., USA, 1984, pp 29-53.
22. Draper, N.R., Smith, H., Applied Regression Analysis 2nd ed., John Wiley & Sons, : New York, 1981, pp.1-125.
23. "Studies on Selective Oxidation of n-butane to maleic-anhydride over Promoted V-P-O Catalyst" Ph.D thesis by S.K. Bej, Department of Chemical Engineering, IIT-Kanpur, April 1991.

24. McBain, J.W., "The Sorption of Gases and Vapour by Solids", George Ruledge and Sons Ltd., London (1932), Ch. 5.
25. Barrer, R.M., Zeolites 1981, 1, 130.
26. Bibby, D.M., and Dale, M.P. Nature 1985, 317, 157.
27. Van Erp, W.A. Kouwenhoven, H.W., and Nanne, J.M. Zeolites 1987, 7, 286.
28. Breck; D.W., Zeolite Molecular Sieves, John Wiley & Sons, New York, 1974.
29. Szostak, R., "Molecular Sieves - Principles of Synthesis and Identification", Van Nostrand Reinhold, New York, 1989.
30. Prabir K. Dutta and Chris Bowers, Zeolites, 1991, Vol. 11, June 507.
31. Scott, J., Zeolite Technology and Applications, recent advances - Chemical Technology Review, No. 170.
32. Grimshaw, Rex W., "The Chemistry and Physics of Clays and allied ceramic materials, 4th ed., London, Ernest Benn, 1971.
33. Zhdanov S.P., "Some Problems of Zeolite crystallization", Adv. chem. Ser. 101 20 (1971).
34. Cho, M., Han, S., Kim, Y., "Crystallization of Zeolite A and HS and Conversion of Zeolite A into Zeolite HS", Hwakak Konghak, 26 : 323, 1988 (Korean) (as cited in Chemical Abstracts, V 110 10607g).
35. Industrial Eng. Chem. Res., Vol. 29, No. 5, 1990 Page (749-754).
36. Francesco Di Renzo and Thierry Des Courieres, Zeolites, 1991, Vol. 11, July/August 539.

APPENDIX

4.1 CHEMICAL ANALYSIS OF DIATOMITE

For chemical analysis of diatomite powdered sample (0.5 gm) was clacined to 4 hours at a temperature of 600°C . The loss of weight was determined and it corresponds to the moisture content in the sample.

A.1.1 ESTIMATION OF SiO_2

The dehydrated sample was mixed with 5 gms of Na_2CO_3 and the mixture was heated in a platinum crucible at 800°C for about 3 hours. The fused mass was then dissolved in dilute HCl and the solution was heated (on a hot plate) for 4-5 hours till a solid mass was obtained, which was once again dissolved in dilute HCl. Fine SiO_2 particles were found to appear. The solution was filtered and the filtrate was heated on hot plate for 4 hours, then dissolved in HCl. This solution was filtered again and the residue was mixed with the already obtained residue of SiO_2 and whole residue was ignited at 800°C in a platinum crucible. The weighing was treated with HF so that SiF_r vaporises and goes out. The wiehgt of crucible with the residue (containing associated $\text{Al}_2\text{O}_3 \cdot \text{Fe}_2\text{O}_3$

etc.) was obtained. The difference between these two weight values corresponds to the amount of silica present in the 0.5 gm of diatomite.

A.1.2 ESTIMATION OF ASSOCIATED OXIDE

The residue that was left on the platinum crucible was then mixed with KHSO_4 and heated on a gas burner. The whole mass was cooled down and mixed in the filtrate (obtained after removal of SiO_2 particles). The mix was subjected to boiling to ensure complete dissolution. After complete dissolution, the whole mass was once again boiled after adding few drops of HNO_3 and 4-5 gms of NH_4Cl to the same. NH_4OH is added to the solution dropwise to precipitate the group-III elements. A white gelatinous precipitate was obtained as soon as the mixture turned alkaline. The solution was filtered on whatman 42 filter paper, reprecipitated with hot ammonical NH_4Cl solution. It was ignited for 2 hours on a gas burner. The weight of this residue after ignition represents the amount of associated oxide.

A.1.3 ESTIMATION OF Fe^{+3}

The residue of associated oxide was mixed with KHSO_4 and fused. The fused mass dissolved in dilute H_2SO_4 solution, and volume made upto 250 ml in volumetric flask. For the estimation of Fe^{+3} by $\text{K}_2\text{Cr}_2\text{O}_7$ titration, 100 ml of this aliquot was taken.

A.1.4 ESTIMATION OF Al_2O_3

The difference of the amount of associated oxide and estimated Fe^{+3} (in form of oxide) corresponds to the amount of Al_2O_3 present 0.5 gm of diatomite.

A.1.5 ESTIMATION OF REST ELEMENTS

The filtrate obtained after precipitation of associated oxide was further analyzed for CaO and MgO by adding ammonium oxalate solution and di-sodium hydrogen phosphate solution respectively. In the present case the estimates obtained of CaO and MgO in the diatomite analyzed was negligible.

A.1.5 ZEOLITE ION EXCHANGE CAPACITY MEASUREMENT IN TERMS OF WATER HARDNESS (CALCIUM & MAGNESIUM ANALYSIS)

1. 25 or 50 ml of hard water was taken in a conical flask.
2. 1-2 ml buffer solution (pH = 10) was added.
3. A pinch of EBT indicator was added and titrated with standard EDTA (0.01 M) till wine red colour changes to blue. The volume of EDTA required (A) was noted down.
4. A blank run was taken, if buffer was not checked properly. The volume of EDTA required for blank run was noted (B).
5. Total volume of EDTA required was calculated $C = A + B$ from volume of EDTA required in 3 and 4 steps.

$$\text{Total hardness mg/litre} = \frac{C \times B \times 1000}{\text{ml of sample}}$$

C = Volume of EDTA required by sample.

$$\begin{aligned} B = \text{mg CaCO}_3 &= 1.0 \text{ ml EDTA } 0.01 \text{ (M)} \\ &= 1.0 \text{ mg of CaCO}_3. \end{aligned}$$

MODEL CALCULATIONS OF % CRYSTALLINITY AND % YIELD :

(Based on Data of run No. 10)

$$\% \text{ Crystallinity} = \frac{\text{Area of the peak of the product}}{\text{Area of the peak of standard sample}} \times 100$$

The Zeolite 4A is taken as standard for this purpose.

$$\% \text{ Crystallinity} = \frac{47.27}{72.495} \times 100 = 65.20$$

$$\% \text{ Yield} = \frac{\text{Molar weight of zeolite A formed}}{\text{Molar weight of aluminosilicate gel fed}} \times 100$$

$$\% \text{ yield} = \frac{25.8}{50} \times 100 = 51.6$$

MODEL CALCULATION OF ANALYSIS OF VARIANCE (ANOVA)

- i) Calculation of Residual Sum of Squares : (based on run no. 1-19)

Run No.	% yield (from experiments)	% yield (from Prediction by Equation)	% yield - % yield expt pred
11	51.24	51.05	0.035
13	50.78	51.93	1.1025
14	50.62	49.97	0.4225
6	50.9	50.86	1.369×10^{-3}
5	50.1	50.29	0.039
12	52.5	52.02	0.2268
10	51.6	50.95	0.4225
16	50.84	51.16	0.1073
8	51.07	50.51	0.3058
4	49.6	50.09	0.2401
7	49.9	49.38	0.265
2	50.08	50.41	0.11055
3	51.3	50.54	0.568
15	50.5	49.33	1.3502
1	47.6	49.47	3.4969
17	51.43	50.95	0.2304
18	51.74	50.95	0.6241
19	51.22	50.95	0.0729

$$\sum (\% \text{ Yield}_{\text{expt}} - \% \text{ Yield}_{\text{Pred}})^2 = 10.005539$$

- ii) Calculations fo Sum of Squares Due to Pure Error (run no. 17 to 19).

The values of Sum of squares due to
pure error = 0.1508686

- iii) Sum of Squares Due to Lack of fit is

$$(10.005539 - 0.1508686) = 9.8546704$$

$$\begin{aligned} \text{iv) } F_{\text{Cal}} &= \frac{\text{Mean square due to lack of fit}}{\text{Mean square due to pure error}} \\ &= \frac{1.0949634}{0.0502895} = 21.773 \end{aligned}$$

$$\text{v) } F_{0.05(9,3)} = 8.81 \text{ is taken from standard F-tables.}$$

MODEL CALCULATION OF ANALYSIS OF VARIANCE (ANOVA)

i) Calculation of Residual Sum of Squares : (based on run numbers 1 to 19)

Run No.	% yield (from experiments)	% yield (from Prediction by Equation)	% yield - % yield expt pred
11	51.24	51.79	0.3125
13	50.78	50.49	0.0841
14	50.62	50.196	0.1797
6	50.9	51.33	0.1849
5	50.1	49.875	0.050625 ₋₃
12	52.5	52.443	3.249×10 ₋₃
9	48.6	48.668	4.624×10 ₋₃
10	51.6	51.5044	9.139×10 ₋₃
16	50.84	50.62	0.0484
8	51.07	51.07138	1.925×10 ₋₆
4	49.6	49.668	4.639×10 ₋₃
7	49.9	49.804	9.216×10 ₋₃
2	50.08	50.639	0.312481
3	51.3	51.014	0.81796
15	50.5	50.08	0.1764
1	47.6	48.028	0.183184 ₋₃
17	51.43	51.5044	5.535×10 ₋₃
18	51.74	51.5044	0.055073
19	51.22	51.5044	0.08088

$$\Sigma (\% \text{ Yield}_{\text{expt}} - \% \text{ Yield}_{\text{Pred}})^2 = 1.7854429.$$

ii) Calculations of Sum of Squares Due to pure error (run No. 17 to 19).

$$\begin{aligned} \text{The values of Sum of squares due to pure error} \\ = 0.1508686 \end{aligned}$$

iii) Sum of Squares Due to Lack-of-fit is
 $(1.7854429 - 0.1508686) = 1.6345743$

$$\text{iv) } F_{\text{Cal}} = \frac{0.1816193}{0.0502895} = 3.61$$

v) $F_{0.05(9,3)} = 8.81$ is taken from standard F-tables.